

The fractional quantum Hall effect: What is the ground state of a two-dimensional electron system at the Landau level filling factor $\nu = 1/3$?

S. A. Mikhailov*

Institute of Physics, University of Augsburg, D-86135 Augsburg, Germany

(Dated: June 15, 2022)

The fractional quantum Hall effect was experimentally discovered in 1982: It was observed that the Hall conductivity of a two-dimensional electron system is quantized, $\sigma_{yx} = e^2/3h$, at the Landau level filling factor $\nu = 1/3$. In 1983, Laughlin proposed a many-body variational wave function, which he claimed described a “new state of matter” – a homogeneous incompressible liquid with fractionally charged quasiparticles. Here we calculate the exact ground state energies and the ground state wave functions of N -particle systems of Coulomb interacting two-dimensional electrons, with N up to $N = 7$, on a compensating positive background having the form of a disk. We also calculate the energy and other physical properties of the Laughlin state for a system of $N \leq 8$ electrons. We show that, while the properties of the exact and Laughlin states are quite close at $N \lesssim 4$ electrons, at larger N they strongly deviate from each other. In particular, at $N \gg 1$ the density of electrons in the Laughlin state takes the form of a ring, with a vanishingly small density in the center and with a very high density near the edge of the positively charged disk. The projection of the Laughlin state on the exact ground state wave function varies from 95% and 91% at $N = 3$ and 4 respectively, down to $\sim 38\%$ at $N = 7$. The true ground state has a substantially lower energy than that of the Laughlin state and has the form of a sliding Wigner crystal.

CONTENTS

I. Introduction	2
II. Formulation and general solution of the problem	4
A. Single-particle problem	4
B. Positive background	5
C. Many-body Hamiltonian	5
D. Basis many-body wave functions	6
E. Many-body matrix elements	7
1. Electron density	8
2. Fourier transform of the electron density	8
3. Background-background interaction energy	8
4. Background-electron interaction energy	8
5. Electron-electron interaction energy	9
6. Pair correlation function	10
F. General solution of the many-body Schrödinger problem	10
III. Two special cases	11
A. The maximum density droplet state	11
B. The classical Wigner crystal configuration	13
IV. Laughlin wave function	15
A. Expansion coefficients of the Laughlin function	15
1. Two particles	16
2. Three particles	16
3. Four particles	16
4. Five to eight particles	18
B. Electron density in the Laughlin state	19
C. Energy of the Laughlin state	20

* Electronic mail: sergey.mikhailov@physik.uni-augsburg.de

V. Exact solution	21
A. The ground state energy and wave function	21
B. The density of electrons in the ground state	23
VI. Conclusions	23
A. Integrals \mathcal{J} and \mathcal{K}	25
B. Supplementary Materials	25
References	25

I. INTRODUCTION

The quantum Hall effect was discovered by Klaus von Klitzing in 1980 [1]. He studied the longitudinal (R_{xx}) and Hall ($R_H = R_{xy}$) resistances of a degenerate two-dimensional (2D) electron gas (EG) in the inversion layer of a Si-MOSFET (metal-oxide-semiconductor field effect transistor). The sample was placed in a strong perpendicular magnetic field $B \approx 18$ T and cooled down to $T \approx 1.5$ K. The resistances R_{xx} and R_{xy} were measured as a function of the gate voltage V_g , applied between the metallic gate and the 2DEG, which changed the density n_s of 2D electrons and the Landau level filling factor

$$\nu = \pi n_s \lambda^2; \quad (1)$$

here

$$\lambda = \sqrt{\frac{2\hbar c}{|e|B}} = \sqrt{\frac{2\hbar}{m\omega_c}} \quad (2)$$

and $\omega_c = |e|B/mc$ is the cyclotron frequency ($\lambda/\sqrt{2}$ is the magnetic length). He found that, when ν is close to integer values $\nu \approx i$, $i = 1, 2, 3, \dots$, the diagonal resistance R_{xx} becomes negligibly small, while the Hall resistance assumes, with a very high accuracy, quantized values, corresponding to the Hall conductivity

$$\sigma_{yx} = \frac{e^2}{h} \nu = \frac{e^2}{h} i, \quad i = 1, 2, 3, \dots \quad (3)$$

The physical origin of this fascinating physical phenomenon, which was called the *integer quantum Hall effect* (IQHE), was quickly understood in terms of the single-particle picture [1]: the classical formula for the Hall conductivity $\sigma_{yx} = n_s e c / B$, together with the relation (1) immediately gives the quantized values (3). The stabilization of σ_{yx} at the levels (3) and the vanishing of σ_{xx} in finite intervals around $\nu = i$ was explained by the influence of disorder, see, e.g., Ref. [2].

The time of mysteries came a little later. In 1982 Tsui, Stormer and Gossard published a paper [3] where the same transport coefficients (R_{xx} and R_{xy}) were measured in another material system, GaAs/AlGaAs heterojunction. The main difference between the new experiment and the one of von Klitzing was that the mobility of 2D electrons was higher ($\mu \sim 10^5$ cm²/Vs) and the temperature was lower (T down to ~ 0.48 K). In the experiment [3] the density of electrons was fixed while the magnetic field varied from zero up to ~ 22 T. Like in Ref. [1], the already familiar integer quantization of R_{xy} was observed around $\nu = 1, 2, 3$, but – very surprisingly – a very similar plateau was found around $\nu \approx 1/3$, where the measured R_H corresponded to the Hall conductivity

$$\sigma_{yx} = \frac{e^2}{h} \nu, \quad \nu = \frac{1}{3}. \quad (4)$$

Subsequent experimental studies showed that such a *fractional* quantization of σ_{yx} and the corresponding suppression of σ_{xx} is the case around many fractions of the form $\nu = p/q$ where p and q are integers and q is odd, see, e.g., Fig. 1 in Ref. [4]. The fractional quantum Hall effect was observed not only in semiconductor structures with a 2D electron gas, but – many years later – also in semimetallic graphene [5].

If $\nu < 1$ all electrons occupy the lowest Landau level, therefore the mysterious feature at $\nu = 1/3$ could not be explained within the single-particle picture. The origin of the fractional quantization had to be searched for within the many-body approach, by taking into account electron-electron interactions. As known, when considered as classical point particles, Coulomb-interacting electrons form the Wigner crystal [6], and Tsui et al. [3] put forward a hypothesis

that the observed $1/3$ feature in the Hall conductivity is related to the formation of the Wigner crystal or a charge density wave state with a triangular symmetry. However, in 1983 Robert Laughlin suggested another idea [7]. He proposed the following variational wave function for the ground state of the N -particle system at $\nu \approx 1/m$:

$$\Psi_{\text{RL}}^m(\mathbf{r}_1, \mathbf{r}_2, \dots, \mathbf{r}_N) \propto \left(\prod_{1 \leq j < k \leq N} (z_j - z_k)^m \right) \exp \left(-\frac{1}{2} \sum_{j=1}^N |z_j|^2 \right), \quad (5)$$

where m is odd integer, $\mathbf{r}_j = (x_j, y_j)$, and $z_j = (x_j - iy_j)/\lambda$ is the normalized complex coordinate of 2D electrons. The function Ψ_{RL}^m is the eigenfunction of the total angular momentum operator with the eigenvalue $\mathcal{L} = mN(N-1)/2$ (in units of \hbar). Laughlin calculated the variational energy of the state (5) and found that at $m = 3$ and 5 it is lower than the charge density wave energy. He also calculated the projection of the wave function (5) onto the lowest-energy eigenstate of the angular momentum \mathcal{L} for three and four particles and found that these projections are close to 1 for $m = 3$ and $m = 5$ states. He concluded that the wave function (5) describes the ground state of the system at $\nu = 1/m$ and characterized it as “a new state of matter”, which is “an incompressible quantum fluid with fractionally charged excitations” [7]. A Wigner crystal alternative was proposed [8], and a few critical comments on the wave function (5) followed [9], but finally the state (5) was accepted by the community [10] as the closest approximation to the ground-state wave function at $\nu = 1/m$.

In this paper we study the ground state properties of a small system of N Coulomb-interacting electrons on a neutralizing positively charged background, having the shape of a disk of the radius $R = \sqrt{N/\pi n_s}$ and the constant areal density n_s . We restrict ourselves by the filling factor $\nu = 1/3$ (i.e., $m = 3$) and the total angular momentum $\mathcal{L} = 3N(N-1)/2$. We calculate the energy and other physical properties of the system for $2 \leq N \leq 7$. Under the assumption that all electrons occupy only the lowest Landau level our results are exact. We also calculate the energy and other physical properties of the Laughlin state (5) for $N \leq 8$ and compare them with the exact results. The comparison shows that the Laughlin wave function (5) is very far from the true ground state of 2D electrons at $\nu = 1/3$, and that the difference increases strongly with the number of particles N .

The simplest way to make sure that the wave function (5) cannot describe the ground state of the considered system is to calculate the density of electrons in the state (5). An inquisitive (or incredulous) reader can easily do this by expanding the factors $(z_j - z_k)^m$ in (5) with the help of the binomial theorem and applying standard quantum-mechanical formulas for the density of electrons, see Section II E 1 for details. The result is shown in Figure 1(b), together with the density of the positive background, Figure 1(a). One sees that the density $n_{\text{RL}}(r)$ of the “Laughlin liquid” (5) is strongly inhomogeneous, has the shape of a ring, with $n_{\text{RL}}(r) \ll n_s$ in the center and $n_{\text{RL}}(r) \gg n_s$ near the edge of the sample. With growing N the ratio $n_{\text{RL}}(r)/n_s$ quickly tends to zero at $r = 0$ and to infinity at $r \simeq R$, see further details of the calculations in Section IV B.

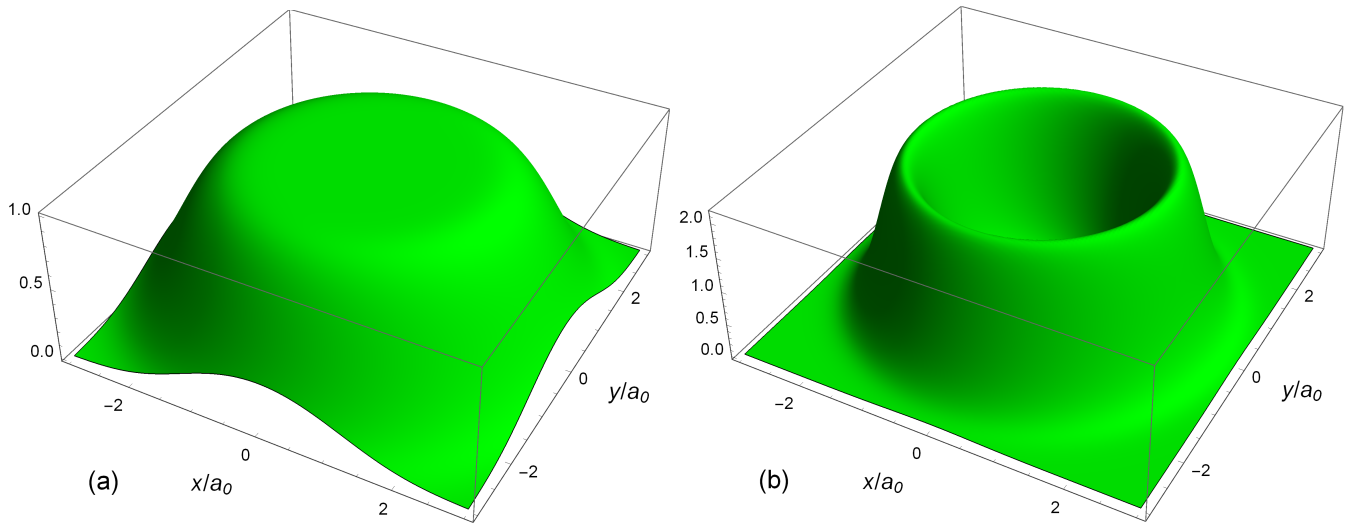


FIG. 1. The densities of (a) the positive background $n_b(r)/n_s$ and (b) the “Laughlin liquid” $n_{\text{RL}}(r)/n_s$ at $m = 3$, as a function of coordinates. The number of particles is $N = 8$; the length scale a_0 is determined by Eq. (13).

In principle, the incorrectness of the Laughlin function (5) had to be expected. The ground state of the system is established as a result of balancing the forces attracting electrons to a positively charged center and repelling them from each other due to the Coulomb interaction. How strongly electrons repel each other is determined, in particular,

by the behavior of a many-body wave function $\Psi(\dots, \mathbf{r}_j, \dots, \mathbf{r}_k \dots)$ at $|\mathbf{r}_j - \mathbf{r}_k| \equiv r_{jk} \rightarrow 0$. Mathematically, this behavior is controlled by the Coulomb interaction term $\sim \Psi/r_{jk}$ in the Schrödinger equation. To compensate the $1/r$ -singularity in this equation, the wave function should be proportional to r_{jk} , and the pair correlation function to r_{jk}^2 at $r_{jk} \rightarrow 0$. This is indeed the case in the maximum density droplet (MDD) state [11] at $\nu = 1$, see Section III A for further details, which is described by the function (5) at $m = 1$. However, for the filling factors $\nu = 1/3$ and $1/5$ Laughlin required $\Psi(\dots, \mathbf{r}_j, \dots, \mathbf{r}_k \dots)$ to be proportional to r_{jk}^3 and r_{jk}^5 at $r_{jk} \rightarrow 0$. This actually suggests that electrons repel each other substantially stronger than needed due to the Coulomb law (this would be a proper choice if electrons repelled each other by the forces proportional to $1/r_{jk}^4$ and $1/r_{jk}^6$, respectively). The pair correlation function would have to be proportional to r_{jk}^6 and r_{jk}^{10} at $r_{jk} \rightarrow 0$, for $m = 3$ and 5 respectively. As a result, the Laughlin electrons “repel” each other too strongly, they do not fit into the potential well of the positive background and accumulate, without need, at the edge of the sample.

The question arises, why the energy calculated by Laughlin for the state (5) was found to be the lowest among other possible trial wave functions? As seen from the paper [7], by analogy with the MDD state at $m = 1$, Laughlin implicitly assumed that the density of electrons in the state (5) is uniform in the thermodynamic limit and perfectly compensate the density of the neutralizing positive background. As a result, he calculated only the correlation contribution to the full Coulomb interaction energy and ignored the Hartree contribution. But in reality, the electron density in the state (5) is strongly inhomogeneous, Figure 1(b), the Hartree energy is nonzero and gives a large positive contribution which substantially grows when N tends to infinity.

The rest of the paper is organized as follows. Section II is preparatory. Here we formulate the problem and discuss all the technical issues needed for the rest of the paper; in particular, we calculate the many-particle matrix elements of the Hamiltonian and of other physical quantities. In Section III we discuss two special cases, the maximum density droplet and the classical Wigner crystal states, which will help to understand the physics of the true ground state of the system in the next sections. Section IV is devoted to the analysis of the Laughlin wave function (5). We calculate the energy and the electron density in the state (5) for the number of particles N varying from $N = 2$ to $N = 8$. All results of this Section are analytical and can be easily verified. In Section V we perform an exact diagonalization study of the problem for $2 \leq N \leq 7$ and analyze the true ground state energy and electron density. In Section VI we summarize our results and formulate the conclusions.

II. FORMULATION AND GENERAL SOLUTION OF THE PROBLEM

A. Single-particle problem

Consider a single 2D electron moving in the plane $z = 0$ in the presence of a uniform external magnetic field $\mathbf{B} = (0, 0, B)$. Its quantum-mechanical motion is described by the single-particle Schrödinger equation

$$\frac{1}{2m} \left(\hat{\mathbf{p}} + \frac{|e|}{2c} \mathbf{B} \times \mathbf{r} \right)^2 \phi(\mathbf{r}) = \epsilon \phi(\mathbf{r}). \quad (6)$$

Its solution,

$$\epsilon \equiv \epsilon_{n,l} = \hbar \omega_c \left(n + \frac{l + |l| + 1}{2} \right), \quad 0 \leq n < \infty, \quad -\infty < l < +\infty, \quad (7)$$

$$\phi(\mathbf{r}) \equiv \phi_{n,l}(\mathbf{r}) = \frac{e^{il\theta}}{\sqrt{2\pi}} \cdot \frac{\sqrt{2}}{\lambda} \left(\frac{n!}{(n + |l|)!} \right)^{1/2} \exp \left(-\frac{r^2}{2\lambda^2} \right) \left(\frac{r}{\lambda} \right)^{|l|} L_n^{|l|} \left(\frac{r^2}{\lambda^2} \right), \quad (8)$$

is characterized by the radial quantum number n and the azimuthal (angular momentum) quantum number l . The functions (8) represent a complete set in a 2D space.

The states with $n = 0$ and non-positive l , $l \leq 0$, belong to the lowest Landau level. The corresponding energy equals $\hbar \omega_c/2$ and the corresponding wave functions are

$$|L\rangle \equiv \psi_L(\mathbf{r}) \equiv \phi_{n=0, l \leq 0}(\mathbf{r}) = \frac{1}{\lambda \sqrt{\pi L!}} \left(\frac{r}{\lambda} e^{-i\theta} \right)^L \exp \left(-\frac{r^2}{2\lambda^2} \right) = \frac{z^L e^{-|z|^2/2}}{\lambda \sqrt{\pi L!}}, \quad (9)$$

where $L = -l = 0, 1, 2, \dots$, and $z = (x - iy)/\lambda$. The states (9) are normalized, $\langle L | L' \rangle = \delta_{LL'}$, and represent a complete subset of functions in two dimensions belonging to the lowest Landau level with $\epsilon_{0,l} = \hbar \omega_c/2$. The matrix elements

of the exponential function $e^{i\mathbf{q}\cdot\mathbf{r}}$ between the single-particle states (9) are

$$\langle L | e^{i\mathbf{q}\cdot\mathbf{r}} | L' \rangle = i^{|L-L'|} e^{i(L-L')\alpha} \sqrt{\frac{(\min\{L, L'\})!}{(\max\{L, L'\})!}} \left(\frac{q\lambda}{2}\right)^{|L-L'|} \exp\left(-\frac{(q\lambda)^2}{4}\right) L_{\min\{L, L'\}}^{|L-L'|} \left(\frac{(q\lambda)^2}{4}\right), \quad (10)$$

where α is the polar angle of the vector \mathbf{q} , $\mathbf{q} = q(\cos \alpha, \sin \alpha)$ and $L_n^l(x)$ are the Laguerre polynomials. We will need the matrix elements (10) below for calculation of some physical properties of N -electron systems.

B. Positive background

N electrons repel each other by Coulomb forces, therefore a compensating positive background is required to keep them together and to ensure the system electroneutrality. We assume that the positive background has the shape of a disk of radius R and is characterized by the uniform density n_s at $r \lesssim R$. The density n_s , the number of electrons N and the disk radius R are related as follows

$$\pi n_s R^2 = N. \quad (11)$$

The positive background density profile $n_b(\mathbf{r})$ can be chosen in different ways. The simplest choice would be to assume the step-like density $n_b(\mathbf{r}) \equiv n_b(r) = n_s \Theta(R-r)$ where $\Theta(x)$ is the Heaviside step function. We prefer to use another, *smooth* density profile, defined as

$$\frac{n_b(r)}{n_s} = e^{-x^2} \sum_{k=0}^{N-1} \frac{x^{2k}}{k!} = \frac{\Gamma(N, x^2)}{\Gamma(N)}, \quad (12)$$

where $x = r/a_0$, $\Gamma(N)$ is the Euler gamma function and $\Gamma(N, x)$ is the incomplete gamma function. The length a_0 is defined as

$$\pi n_s a_0^2 = 1 \quad (13)$$

and will be used as the length unit throughout the paper. Notice that it does not depend on B . This choice is more convenient than in [7] (where the magnetic length was used as the length unit), since it enables to analyze the system behavior at varying magnetic fields.

The function (12) is shown in Figure 2 for $N = 100$, together with the step-like profile. One sees that it is equal to unity in the area $r \lesssim R$ and is smoothed near the edge of the disk at the length $\sim a_0$. In fact, the function $n_b(\mathbf{r})$ gives a more realistic description of the actual density profile, since in real systems the edge is always smoothed over a certain length, for example, the distance between the 2D gas and the donor layer in GaAs/AlGaAs heterostructures or the inter-particle distance a_0 . The function $n_b(\mathbf{r})$ satisfies the condition

$$\int n_b(\mathbf{r}) d\mathbf{r} = N. \quad (14)$$

The Fourier transform of the function (12) is given by the formula

$$n_{\mathbf{q}}^b = \int d\mathbf{r} n_b(\mathbf{r}) e^{i\mathbf{q}\cdot\mathbf{r}} = e^{-Z} L_{N-1}^1(Z), \quad (15)$$

where $Z = (qa_0/2)^2$. We will need the Fourier transform (15) below for calculating some physical properties of the considered system.

C. Many-body Hamiltonian

The Hamiltonian of N interacting 2D electrons, placed in the attractive potential of the positive background (12) and in the magnetic field $\mathbf{B} = (0, 0, B)$, has the form

$$\hat{\mathcal{H}} = \hat{K} + \hat{V}_C = \frac{1}{2m} \sum_{j=1}^N \left(\hat{\mathbf{p}}_j + \frac{|e|}{2c} \mathbf{B} \times \mathbf{r}_j \right)^2 + \hat{V}_C. \quad (16)$$

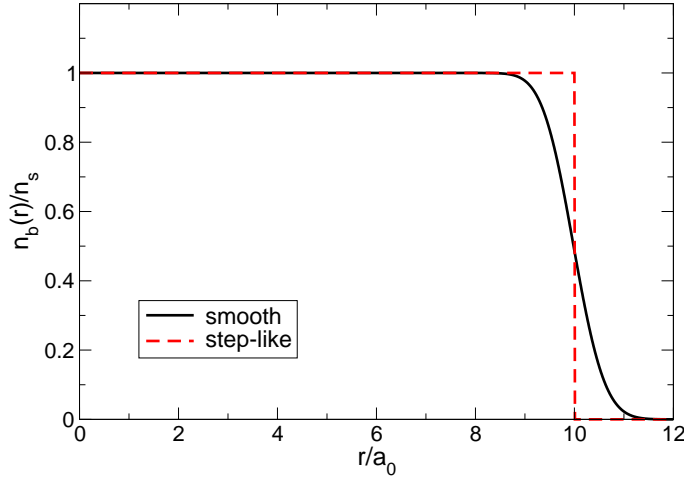


FIG. 2. The positive background density $n_b(r)$ for $N = 100$ in the smooth and step-like profile models.

Here \hat{K} is the total kinetic energy operator and the Coulomb interaction energy \hat{V}_C consists of the sum of background-background, background-electron and electron-electron interaction energies,

$$\hat{V}_C = \hat{V}_{bb} + \hat{V}_{eb} + \hat{V}_{ee} = \frac{e^2}{2} \int \frac{n_b(\mathbf{r})n_b(\mathbf{r}')d\mathbf{r}d\mathbf{r}'}{|\mathbf{r} - \mathbf{r}'|} - e^2 \int n_b(\mathbf{r})d\mathbf{r} \sum_{j=1}^N \frac{1}{|\mathbf{r} - \mathbf{r}_j|} + \frac{e^2}{2} \sum_{j \neq k=1}^N \frac{1}{|\mathbf{r}_j - \mathbf{r}_k|}. \quad (17)$$

In order to calculate the energy \hat{V}_C it is convenient to rewrite (17) in terms of Fourier transforms of the Coulomb potential and of the background charge density. This gives

$$\hat{V}_C = \frac{e^2}{2\pi} \int \frac{d\mathbf{q}}{q} \left(\frac{1}{2} (n_{\mathbf{q}}^b)^2 - n_{\mathbf{q}}^b \sum_{j=1}^N e^{-i\mathbf{q} \cdot \mathbf{r}_j} + \frac{1}{2} \sum_{j \neq k=1}^N e^{i\mathbf{q} \cdot \mathbf{r}_j} e^{-i\mathbf{q} \cdot \mathbf{r}_k} \right), \quad (18)$$

where $n_{\mathbf{q}}^b$ is given by Eq. (15). The Hamiltonian (16) commutes with the total angular momentum operator

$$\hat{\mathcal{L}}_z = \sum_{j=1}^N (\mathbf{r}_j \times \hat{\mathbf{p}}_j)_z. \quad (19)$$

The total angular momentum quantum number $\mathcal{L} \equiv \mathcal{L}_z$ can be used to classify the many-body basis wave functions.

D. Basis many-body wave functions

Consider N electrons at the lowest Landau level. Each of the particles can occupy one of the states (9). If the j -th particle is in the single-particle state $|L_j\rangle = \psi_{L_j}(\mathbf{r})$, the corresponding many-body wave function can be written as a Slater determinant

$$|L_1, L_2, \dots, L_N\rangle = \frac{1}{\sqrt{N!}} \begin{vmatrix} \psi_{L_1}(\mathbf{r}_1) & \psi_{L_1}(\mathbf{r}_2) & \dots & \psi_{L_1}(\mathbf{r}_N) \\ \psi_{L_2}(\mathbf{r}_1) & \psi_{L_2}(\mathbf{r}_2) & \dots & \psi_{L_2}(\mathbf{r}_N) \\ \dots & \dots & \dots & \dots \\ \psi_{L_N}(\mathbf{r}_1) & \psi_{L_N}(\mathbf{r}_2) & \dots & \psi_{L_N}(\mathbf{r}_N) \end{vmatrix}. \quad (20)$$

The functions (20) are orthogonal and normalized,

$$\langle L'_1, L'_2, \dots, L'_N | L_1, L_2, \dots, L_N \rangle = \delta_{L'_1 L_1} \delta_{L'_2 L_2} \dots \delta_{L'_N L_N}. \quad (21)$$

They are eigenfunctions of the kinetic energy operator

$$\hat{K} |L_1, L_2, \dots, L_N\rangle = N \frac{\hbar \omega_c}{2} |L_1, L_2, \dots, L_N\rangle, \quad (22)$$

and of the total angular momentum operator $\hat{\mathcal{L}}$

$$\hat{\mathcal{L}}_z |L_1, L_2, \dots, L_N\rangle = \left(\sum_{i=1}^N L_i \right) |L_1, L_2, \dots, L_N\rangle, \quad (23)$$

where the latter is measured in units of \hbar . The many-body wave functions (20) represent the orthonormal basis set of functions belonging to the lowest Landau level.

If N electrons occupy the single-particle states with the lowest possible angular momenta L from $L = 0$ up to $L = N - 1$, one gets the many-body configuration $\Psi_{\text{mdd}} = |0, 1, 2, \dots, N-1\rangle$ which is often referred to as the maximum density droplet (MDD) state. This MDD configuration has the lowest possible total angular momentum

$$\mathcal{L} = \mathcal{L}_{\min} = \sum_{L=0}^{N-1} L = \frac{N(N-1)}{2}. \quad (24)$$

If $\mathcal{L} > \mathcal{L}_{\min}$, there are, in general, more than one many-body electronic configurations corresponding to the given N and \mathcal{L} . For example, Tables I and II show all possible many-body configurations for $N = 2$ and $N = 3$ and several \mathcal{L} . The number $N_{\text{mbs}}(N, \mathcal{L})$ of many-body configurations with the given N and \mathcal{L} grows with \mathcal{L} for a given N .

TABLE I. Possible many-body configurations in a system of $N = 2$ electrons. N_{mbs} is the total number of all many-particle configurations.

\mathcal{L}	Configurations	N_{mbs}
1	$ 0, 1\rangle$	1
2	$ 0, 2\rangle$	1
3	$ 0, 3\rangle 1, 2\rangle$	2
4	$ 0, 4\rangle 1, 3\rangle$	2
5	$ 0, 5\rangle 1, 4\rangle 2, 3\rangle$	3
6	$ 0, 6\rangle 1, 5\rangle 2, 4\rangle$	3
7	$ 0, 7\rangle 1, 6\rangle 2, 5\rangle 3, 4\rangle$	4

TABLE II. Possible many-body configurations in a system of $N = 3$ particles. N_{mbs} is the total number of all many-particle configurations.

\mathcal{L}	Configurations	N_{mbs}
3	$ 0, 1, 2\rangle$	1
4	$ 0, 1, 3\rangle$	1
5	$ 0, 1, 4\rangle 0, 2, 3\rangle$	2
6	$ 0, 1, 5\rangle 0, 2, 4\rangle 1, 2, 3\rangle$	3
7	$ 0, 1, 6\rangle 0, 2, 5\rangle 0, 3, 4\rangle 1, 2, 4\rangle$	4
8	$ 0, 1, 7\rangle 0, 2, 6\rangle 0, 3, 5\rangle 1, 2, 5\rangle 1, 3, 4\rangle$	5
9	$ 0, 1, 8\rangle 0, 2, 7\rangle 0, 3, 6\rangle 0, 4, 5\rangle 1, 2, 6\rangle 1, 3, 5\rangle 2, 3, 4\rangle$	7

E. Many-body matrix elements

For calculation of different physical properties of an N -electron system we will need matrix elements of one-particle or two-particle operators,

$$\langle L'_1, L'_2, \dots, L'_N | \sum_{j=1}^N \hat{F}_1(\mathbf{r}_j) |L_1, L_2, \dots, L_N\rangle, \quad (25)$$

$$\langle L'_1, L'_2, \dots, L'_N | \sum_{j=1}^N \sum_{k=1, k \neq j}^N \hat{F}_2(\mathbf{r}_j, \mathbf{r}_k) |L_1, L_2, \dots, L_N\rangle, \quad (26)$$

with the many-body states (20). In this paper we consider only the ground state properties of the system. In this case we will need only the matrix elements (25)–(26) between the many-body states $\langle \{L'_j\} |$ and $|\{L_j\}\rangle$, belonging to the same total angular momentum \mathcal{L} , i.e., $\sum_{j=1}^N L_j = \sum_{j=1}^N L'_j = \mathcal{L}$. This means that, if the bra and ket configurations are different, they differ by two or more single-particle states, for example, $\langle 0, 1, 8 |$ and $|0, 2, 7\rangle$, $\langle 0, 3, 6 |$ and $|1, 3, 5\rangle$ (configurations differ by two single-particle states), $\langle 0, 1, 8 |$ and $|2, 3, 4\rangle$ (configurations differ by three single-particle states), etc., see Table II. The matrix elements between the bra and ket configurations which differ by only one single-particle state, e.g., between the configurations $\langle 0, 1, 8 |$ and $|0, 1, 9\rangle$, will not be considered since they correspond to different values of the total angular momentum \mathcal{L} .

Now we calculate matrix elements of several one-particle and two-particle operators of the type (25)–(26). For brevity we will use the short notations $|s\rangle \equiv |\Psi_s\rangle \equiv |L_1^{(s)}, L_2^{(s)}, \dots, L_N^{(s)}\rangle$ for the functions (20).

1. Electron density

The operator of the electron density has the form

$$\hat{n}_e(\mathbf{r}) = \sum_{j=1}^N \delta(\mathbf{r} - \mathbf{r}_j). \quad (27)$$

The off-diagonal matrix elements of (27) are evidently zero. Then we get

$$\langle \Psi_s | \hat{n}_e(\mathbf{r}) | \Psi_{s'} \rangle = \delta_{ss'} \sum_{j=1}^N \langle L_j^{(s)} | \delta(\mathbf{r} - \mathbf{r}_j) | L_j^{(s')} \rangle = \delta_{ss'} \sum_{j=1}^N |\psi_{L_j^{(s)}}(\mathbf{r})|^2, \quad (28)$$

where $\psi_{L_j^{(s)}}(\mathbf{r})$ is the ψ -function of the j -th particle in the s -th many-body configuration.

2. Fourier transform of the electron density

The Fourier transform of the density operator (27) is

$$\hat{n}_{\mathbf{q}}^e = \int d\mathbf{r} \hat{n}_e(\mathbf{r}) e^{i\mathbf{q} \cdot \mathbf{r}} = \sum_{j=1}^N e^{i\mathbf{q} \cdot \mathbf{r}_j}. \quad (29)$$

Using Eq. (10) we get

$$\langle \Psi_s | \hat{n}_{\mathbf{q}}^e | \Psi_{s'} \rangle = \delta_{ss'} \sum_{j=1}^N \langle L_j^{(s)} | e^{i\mathbf{q} \cdot \mathbf{r}_j} | L_j^{(s')} \rangle = \delta_{ss'} \exp\left(-\frac{(q\lambda)^2}{4}\right) \sum_{j=1}^N L_j^0 \left(\frac{(q\lambda)^2}{4}\right). \quad (30)$$

3. Background-background interaction energy

The background-background interaction energy V_{bb} is given by the first term in Eq. (18). Since V_{bb} is constant (does not depend on the coordinates of electrons), the matrix $\langle \Psi_s | \hat{V}_{bb} | \Psi_{s'} \rangle$ is diagonal and all nonzero matrix elements are the same. They can be expressed in terms of the integral $\mathcal{J}(n_1, n_2, l_1, l_2, k; \alpha, \beta)$ defined in Appendix A, see Eqs. (A1) and (A3). Substituting (15) in the first term of Eq. (18) we obtain

$$\langle \Psi_s | \hat{V}_{bb} | \Psi_{s'} \rangle = \delta_{ss'} \frac{e^2}{a_0} \sqrt{\frac{\pi}{8}} \mathcal{J}(N-1, N-1, 1, 1, 0; 1, 1). \quad (31)$$

4. Background-electron interaction energy

The background-electron interaction energy is given by the second term in Eq. (18). Its many-body matrix elements are

$$\langle \Psi_s | \hat{V}_{be} | \Psi_{s'} \rangle = -\frac{e^2}{2\pi} \int \frac{d\mathbf{q}}{q} n_{\mathbf{q}}^b \langle \Psi_s | (\hat{n}_{\mathbf{q}}^e)^* | \Psi_{s'} \rangle. \quad (32)$$

Substituting here the Fourier transforms of the background and electron densities from Eqs. (15) and (30) we obtain

$$\langle \Psi_s | \hat{V}_{be} | \Psi_{s'} \rangle = -\delta_{ss'} \frac{e^2}{a_0} 2\sqrt{\beta} \int_0^\infty dx e^{-x^2(1+\beta)} L_{N-1}^1(x^2\beta) \sum_{j=1}^N L_{L_j^{(s)}}^0(x^2), \quad (33)$$

where

$$\beta = \frac{a_0^2}{\lambda^2} = \frac{1}{\nu} \quad (34)$$

is the inverse Landau level filling factor. Comparing this result with the definition of the integral \mathcal{J} , Eq. (A1), we finally get

$$\langle \Psi_s | \hat{V}_{be} | \Psi_{s'} \rangle = -\delta_{ss'} \frac{e^2}{a_0} \sqrt{\frac{\pi\beta}{2}} \sum_{j=1}^N \mathcal{J}(L_j^{(s)}, N-1, 0, 1, 0; 1, \beta). \quad (35)$$

The matrix elements (35) depend on the magnetic field B .

5. Electron-electron interaction energy

The electron-electron interaction energy is given by the third term in Eq. (18). Calculating its many-body matrix elements we get the following results:

$$\langle \Psi_s | \hat{V}_{ee} | \Psi_{s'} \rangle = \delta_{ss'} (V_{ss}^H - V_{ss}^F) + (1 - \delta_{ss'}) V_{ss'}^{\text{off}}. \quad (36)$$

The diagonal matrix elements ($s = s'$) are given by the difference of Hartree and Fock contributions, which can be written in terms of the integrals \mathcal{K} defined in Eq. (A4):

$$V_{ss}^H = \frac{e^2}{a_0} \sqrt{\frac{\pi\beta}{8}} \sum_{j=1}^N \sum_{k=1}^N \mathcal{K}(L_j^{(s)}, L_k^{(s)}, 0), \quad (37)$$

$$V_{ss}^F = \frac{e^2}{a_0} \sqrt{\frac{\pi\beta}{8}} \sum_{j=1}^N \sum_{k=1}^N \mathcal{K}(L_{\min}, L_{\min}, \delta L). \quad (38)$$

where in the last formula

$$L_{\min} = \min\{L_j^{(s)}, L_k^{(s)}\}, \quad L_{\max} = \max\{L_j^{(s)}, L_k^{(s)}\}, \quad \delta L = |L_j^{(s)} - L_k^{(s)}| = L_{\max} - L_{\min}. \quad (39)$$

The formulation of results for the off-diagonal matrix elements ($s \neq s'$) requires a bit longer discussion. First, since $s \neq s'$, the sets of numbers L_j^s and $L_j^{s'}$, $j = 1, 2, \dots, N$, differ from each other. In general, these sets may differ by one, two or more numbers. The case when they differ by only one number is excluded, since both sets should satisfy the total angular momentum conservation condition. If they differ by more than two numbers, the corresponding matrix element equals zero,

$$\langle \Psi_s | \hat{V}_{ee} | \Psi_{s'} \rangle = 0, \text{ if the sets } L_j^s \text{ and } L_j^{s'} \text{ differ by more than two numbers.} \quad (40)$$

Thus, the matrix elements $\langle \Psi_s | \hat{V}_{ee} | \Psi_{s'} \rangle$ are nonzero if and only if the states $|s\rangle$ and $|s'\rangle$ differ from each other by the single-particle states of exactly two particles. For example, for three particles with the total angular momentum $\mathcal{L} = 9$, Table II, the matrix elements

$$\langle 0, 2, 7 | \hat{V}_{ee} | 0, 4, 5 \rangle \text{ and } \langle 0, 1, 8 | \hat{V}_{ee} | 1, 2, 6 \rangle \quad (41)$$

are finite (only two numbers in the bra and ket configurations are different), but the matrix element

$$\langle 0, 2, 7 | \hat{V}_{ee} | 1, 3, 5 \rangle \quad (42)$$

is zero (all three numbers are different).

Let the configurations

$$|s\rangle = |\dots, \underbrace{L_1^s}_{p_1^s}, \dots, \underbrace{L_2^s}_{p_2^s}, \dots\rangle \text{ and } |s'\rangle = |\dots, \underbrace{L_1^{s'}}_{p_1^{s'}}, \dots, \underbrace{L_2^{s'}}_{p_2^{s'}}, \dots\rangle \quad (43)$$

differ from each other by the L -states of exactly two particles. We designate them as L_1^s, L_2^s and $L_1^{s'}, L_2^{s'}$, and their serial numbers in the sets $|s\rangle$ and $|s'\rangle$ as $p_1^s, p_2^s, p_1^{s'}, p_2^{s'}$; all other states in (43), designated by dots, are identical. For example, for the first of the matrix elements in (41), $\langle 0, 2, 7 | \hat{V}_{ee} | 0, 4, 5 \rangle$, these numbers are $L_1^s = 2, L_2^s = 7, p_1^s = 2, p_2^s = 3$, and $L_1^{s'} = 4, L_2^{s'} = 5, p_1^{s'} = 2, p_2^{s'} = 3$. For the second matrix element in (41), $\langle 0, 1, 8 | \hat{V}_{ee} | 1, 2, 6 \rangle$, they are $L_1^s = 0, L_2^s = 8, p_1^s = 1, p_2^s = 3$, and $L_1^{s'} = 2, L_2^{s'} = 6, p_1^{s'} = 2, p_2^{s'} = 3$.

Now we can formulate the results for the off-diagonal matrix elements of the electron-electron interaction energy. Calculations show that

$$V_{ss'}^{\text{off}} = \frac{e^2}{a_0} \sqrt{\frac{\pi\beta}{2}} (-1)^{p_1^s + p_2^s + p_1^{s'} + p_2^{s'}} \times \left[\mathcal{K} \left(\min\{L_1^s, L_1^{s'}\}, \min\{L_2^s, L_2^{s'}\}, |L_1^s - L_1^{s'}| \right) - \mathcal{K} \left(\min\{L_1^s, L_2^{s'}\}, \min\{L_2^s, L_1^{s'}\}, |L_1^s - L_2^{s'}| \right) \right] \quad s \neq s', \quad (44)$$

where the integrals \mathcal{K} defined in Eq. (A4).

Equations (36), (37), (38) and (44) give the matrix elements of the electron-electron interaction between the basis many-body configurations (20). Notice that the magnetic field enters these formulas only via the common prefactor $\sqrt{\beta}$.

6. Pair correlation function

The pair correlation function is defined as

$$\hat{P}(\mathbf{r}, \mathbf{r}') = \sum_{j=1}^N \sum_{k=1, k \neq j}^N \delta(\mathbf{r} - \mathbf{r}_j) \delta(\mathbf{r} - \mathbf{r}_k). \quad (45)$$

Its diagonal and off-diagonal matrix elements are determined by the following formulas,

$$\langle \Psi_s | \hat{P}(\mathbf{r}, \mathbf{r}') | \Psi_s \rangle = \sum_{j=1}^N \sum_{k=1}^N \left(|\psi_{L_j^{(s)}}(\mathbf{r})|^2 |\psi_{L_k^{(s)}}(\mathbf{r}')|^2 - \psi_{L_j^{(s)}}^*(\mathbf{r}) \psi_{L_k^{(s)}}(\mathbf{r}) \psi_{L_j^{(s)}}(\mathbf{r}') \psi_{L_k^{(s)}}^*(\mathbf{r}') \right), \quad (46)$$

$$\langle \Psi_s | \hat{P}(\mathbf{r}, \mathbf{r}') | \Psi_{s'} \rangle = (-1)^{p_1^s + p_2^s + p_1^{s'} + p_2^{s'}} \left(\psi_{L_1^s}^*(\mathbf{r}) \psi_{L_2^s}^*(\mathbf{r}') \det \begin{vmatrix} \psi_{L_1^{s'}}(\mathbf{r}) & \psi_{L_2^{s'}}(\mathbf{r}) \\ \psi_{L_1^{s'}}(\mathbf{r}') & \psi_{L_2^{s'}}(\mathbf{r}') \end{vmatrix} + (\mathbf{r} \leftrightarrow \mathbf{r}') \right), \quad s \neq s', \quad (47)$$

where the numbers $L_1^s, L_2^s, L_1^{s'}, L_2^{s'}$, as well as $p_1^s, p_2^s, p_1^{s'}, p_2^{s'}$ have the same meaning as in the previous section.

F. General solution of the many-body Schrödinger problem

Consider the N -particle Schrödinger equation

$$\hat{\mathcal{H}}\Psi(\mathbf{r}_1, \mathbf{r}_2, \dots, \mathbf{r}_N) = E\Psi(\mathbf{r}_1, \mathbf{r}_2, \dots, \mathbf{r}_N). \quad (48)$$

In order to solve it at a given angular momentum \mathcal{L} the function Ψ should be searched in the form of the linear combination of all many-body states corresponding to the given values of N and \mathcal{L} ,

$$|\Psi\rangle = \sum_{s'=1}^{N_{\text{mbs}}} A_{s'} |\Psi_{s'}\rangle. \quad (49)$$

Here s enumerates all N_{mbs} possible many-body configurations with the given N and \mathcal{L} , and A_s are unknown numbers. Substituting (49) into (48) and multiplying the resulting equation by $\langle \Psi_s |$ we reduce the Schrödinger problem to the matrix equation

$$\sum_{s'=1}^{N_{mbs}} \langle \Psi_s | \hat{\mathcal{H}} | \Psi_{s'} \rangle A_{s'} = EA_s. \quad (50)$$

The size of the Hamiltonian matrix $\mathcal{H}_{ss'} \equiv \langle \Psi_s | \hat{\mathcal{H}} | \Psi_{s'} \rangle$ here is $N_{mbs} \times N_{mbs}$, where $N_{mbs}(N, \mathcal{L})$ depends on N and \mathcal{L} . Solving the eigenvalue problem (50) we can find N_{mbs} solutions for any given N and \mathcal{L} : the energies $E_{N, \mathcal{L}, k}$ and the sets of numbers $A_s^{N, \mathcal{L}, k}$, $k = 1, \dots, N_{mbs}$, which give the corresponding many-body wave functions according to the expansion (49). The ground and excited states (for the given values of N and \mathcal{L}) corresponds to $k = 1$ and $k > 1$, respectively.

After the numbers $A_s^{N, \mathcal{L}, k}$ are found we can also calculate all physical properties of the ground or excited many-body states, for example, the electron density and the pair correlation function, using the corresponding matrix elements found in Section II E.

The matrix elements of the Hamiltonian $\mathcal{H}_{ss'} = K_{ss'} + V_{ss'}^C$ are given by the sum of the kinetic $K_{ss'} = \delta_{ss'} N \hbar \omega_c / 2$ and Coulomb energy $V_{ss'}^C = \langle \Psi_s | \hat{V}_{bb} + \hat{V}_{be} + \hat{V}_{ee} | \Psi_{s'} \rangle$ matrix elements. All results for $V_{ss'}^C$ are expressed in terms of the integral \mathcal{J} , Eqs. (A1) and (A3), therefore we can get, at least in principle, *exact analytical* results for the energies and wave functions of the N -electron system at any \mathcal{L} . In practice, of course, the computation time becomes too large if N or \mathcal{L} are much greater than one. Nevertheless, the ground state physics of a fractional quantum Hall system can be quite well understood even if the number of particles is less than or of the order of ten. In Section V below we show results for a quite macroscopic number $N = 7$ and for $\mathcal{L} = 3\mathcal{L}_{\min} = 63$, which corresponds to the Landau level filling factor $\nu = 1/3$. The number of basis many-body configurations in this case, $N_{mbs}(N, \mathcal{L}) = N_{mbs}(7, 63) = 8033$ is not extremely large, which allows to calculate the matrix elements $\mathcal{H}_{ss'}$ and to diagonalize the Hamiltonian matrix within reasonable computation time.

Now we can discuss some results of the theory obtained with the help of formulas derived above.

III. TWO SPECIAL CASES

We begin with two simple special cases which will help us to better understand the physics of the exact solution and the problems of the Laughlin wave function (5).

A. The maximum density droplet state

Let us consider N particles in the many-body state with the lowest total angular momentum $\mathcal{L} = \mathcal{L}_{\min} = N(N-1)/2$, Eq. (24). The number of many-body configurations in this case is $N_{mbs}(N, \mathcal{L}_{\min})$ equals one, and the corresponding wave function is

$$\Psi_{\text{mdd}} = |0, 1, 2, \dots, N-1\rangle = \frac{1}{\sqrt{N!}} \begin{vmatrix} \psi_0(\mathbf{r}_1) & \psi_0(\mathbf{r}_2) & \dots & \psi_0(\mathbf{r}_N) \\ \psi_1(\mathbf{r}_1) & \psi_1(\mathbf{r}_2) & \dots & \psi_1(\mathbf{r}_N) \\ \dots & \dots & \dots & \dots \\ \psi_{N-1}(\mathbf{r}_1) & \psi_{N-1}(\mathbf{r}_2) & \dots & \psi_{N-1}(\mathbf{r}_N) \end{vmatrix}. \quad (51)$$

This *maximum density droplet* state is considered to be the ground state of the system at $\nu = 1$, Ref. [11]. It really gives the lowest energy at $\nu = 1$ if to consider only the lowest Landau level states for forming the many-body configurations. Since $\psi_L(\mathbf{r})$ is proportional to z^L , the function (51) coincides with the Vandermonde determinant and can therefore be presented in the form (5) with $m = 1$, $\Psi_{\text{mdd}} \propto [\prod_{j < k} (z_j - z_k)] \exp(-\sum_j |z_j|^2/2)$.

The density of electrons in the state (51) at $\nu = 1$, according to (28), is

$$n_e^{\text{mdd}}(\mathbf{r}) = \sum_{L=0}^{N-1} |\psi_L(\mathbf{r})|^2 = \frac{1}{\pi \lambda^2} e^{-r^2/\lambda^2} \sum_{L=0}^{N-1} \frac{(r/\lambda)^{2L}}{L!} = n_s \frac{\Gamma(N, r^2/a_0^2)}{\Gamma(N)}, \quad (52)$$

where in the last formula we take into account that, if $\nu = 1$ then $\lambda = a_0$. The electron density (52) coincides with the background density (12), see Fig. 2. At $N \rightarrow \infty$ the density (52) becomes uniform in the whole 2D space, $n_e^{\text{mdd}}(\mathbf{r}) = n_s$.

The pair correlation function (45) of the N -electron configuration (51) at $\nu = 1$ can be presented in the form

$$P_{\text{mdd}}(\mathbf{r}, \mathbf{r}') = n_e^{\text{mdd}}(\mathbf{r}) n_e^{\text{mdd}}(\mathbf{r}') - n_s^2 e^{-|z-z'|^2} \frac{\Gamma(N, zz'^*)}{\Gamma(N)} \frac{\Gamma(N, z^* z')}{\Gamma(N)} \equiv n_e^{\text{mdd}}(\mathbf{r}) n_e^{\text{mdd}}(\mathbf{r}') - \delta P_{\text{mdd}}(\mathbf{r}, \mathbf{r}'). \quad (53)$$

The dependence of $P_{\text{mdd}}(\mathbf{r}, \mathbf{r}')$ on x/a_0 and y/a_0 at $\mathbf{r}'/a_0 = (0, 0)$ and $\mathbf{r}'/a_0 = (3, 0)$ for $N = 30$ particles is shown in Fig. 3. The pair correlation function tends to unity when $|\mathbf{r} - \mathbf{r}'|/a_0 \gg 1$ and both points, \mathbf{r} and \mathbf{r}' , are far from the system boundaries. In the limit $|\mathbf{r} - \mathbf{r}'| \rightarrow 0$ the function $P_{\text{mdd}}(\mathbf{r}, \mathbf{r}')$ tends to zero as $|\mathbf{r} - \mathbf{r}'|^2$, due to the exchange “interaction”.

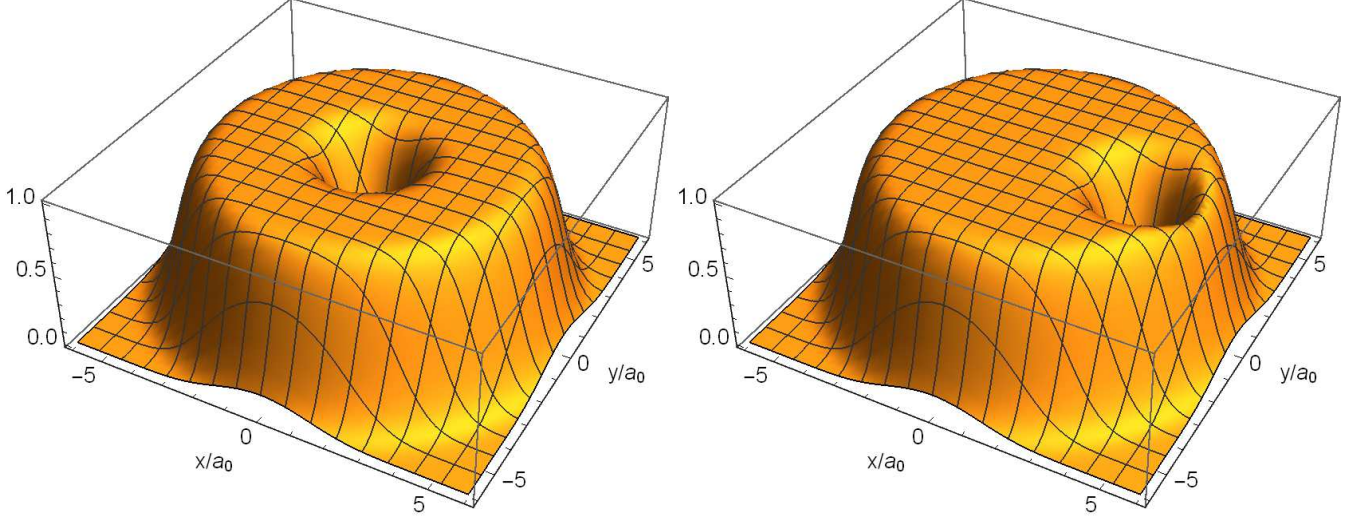


FIG. 3. The pair correlation function of the MDD state (51), a function of \mathbf{r}/a_0 , at $N = 30$ and $\mathbf{r}'/a_0 = (0, 0)$ and $\mathbf{r}'/a_0 = (3, 0)$.

In the limit $N \rightarrow \infty$ the pair correlation function (53) assumes the form

$$P_{\text{mdd}}(\mathbf{r}, \mathbf{r}') = n_s^2 \left(1 - e^{-|\mathbf{r} - \mathbf{r}'|^2/a_0^2} \right). \quad (54)$$

In this limit the function (54) depends only on the distance between the particles.

Consider the energy of the configuration (51). Since the electron and background densities are identical in this state, the background-background, electron-background, and Hartree contributions to the total energy E_{mdd} cancel out, so that one finally gets only the Fock contribution (at $\beta = 1$),

$$E_{\text{mdd}}(N) = -\frac{e^2}{a_0} \sqrt{\frac{\pi}{8}} \sum_{L=0}^{N-1} \sum_{L'=0}^{N-1} \frac{L_{\min}!}{L_{\max}!} \mathcal{J}(L_{\min}, L_{\min}, \delta L, \delta L, \delta L; 1, 1); \quad (55)$$

here $L_{\min} = \min\{L, L'\}$, $L_{\max} = \max\{L, L'\}$, and $\delta L = |L - L'|$. The energy (55) can be also presented in terms of the pair correlation function (53),

$$E_{\text{mdd}}(N) = -\frac{e^2}{2} \int \frac{d\mathbf{r} d\mathbf{r}'}{|\mathbf{r} - \mathbf{r}'|} \delta P_{\text{mdd}}(\mathbf{r}, \mathbf{r}') = -\frac{e^2}{a_0} \frac{1}{2\pi^2} \int \frac{d\mathbf{r} d\mathbf{r}'}{|\mathbf{r} - \mathbf{r}'|} \frac{e^{-|\mathbf{r} - \mathbf{r}'|^2} \Gamma(N, zz'^*) \Gamma(N, z^* z')}{\Gamma^2(N)} \quad (56)$$

where the variables \mathbf{r} and \mathbf{r}' in the second formula are dimensionless. The energy (56) is negative, and its absolute values linearly grows with N at $N \rightarrow \infty$. Figure 4 shows the energy per particle $E_{\text{mdd}}(N)/N$ as a function of the number of electrons N . The red arrow in Fig. 4 shows the asymptotic value $\lim_{N \rightarrow \infty} E_{\text{mdd}}(N)/N = -\sqrt{\pi}/2$, in units of e^2/a_0 , reported in Ref. [7]. As seen from Figure 4, the energy converges to its asymptotic value rather slowly with N : at $N = 100$ the deviation is still about 3.58%.

It is important to emphasize that the total Coulomb energy of the MDD configuration could be reduced to the Fock energy only because the density of electrons and the density of the positive background are identical at all \mathbf{r} and at all values of N . If this was not the case, the background-background, electron-background, and Hartree contributions would not compensate each other and would give a positive contribution to the total energy of the system.

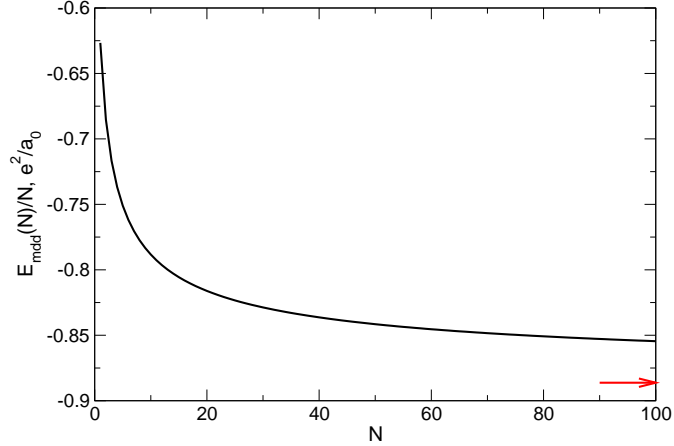


FIG. 4. The energy per particle of the MDD state (51), measured in units e^2/a_0 , as a function of the number of electrons N . The red arrow shows the asymptotic value $[E_{\text{mdd}}(N)/N]_{N \rightarrow \infty} = -\sqrt{\pi}/2$, reported in Ref. [7].

B. The classical Wigner crystal configuration

The MDD wave function (51) describes a quantum state with an ideally uniform electron density (even in a finite- N system) and a uniform (except the exchange hole at $|\mathbf{r} - \mathbf{r}'| \rightarrow 0$) correlation function. It can be characterized as a liquid state in which the Coulomb correlations are completely ignored. What should be expected in the opposite case when the Coulomb interaction effects are strong? To answer this question we consider the limiting case of a system of N (≤ 8) point charged particles forming the Wigner molecule.

If N charged particles are placed in the attractive potential of the positive background with the density (12), they repel each other and can form two types of Wigner molecules, Fig. 5: with a single shell, when all N particles are located on a ring of a finite radius R_s , Figs. 5(a)-5(e), and with two shells, when one particle is at the center of the positive background disk, and $N - 1$ particles are located on a ring around the center, Figs. 5(f)-5(h). To understand which of the two possibilities actually takes place, one should calculate the total energy of the Wigner molecules in both situations.

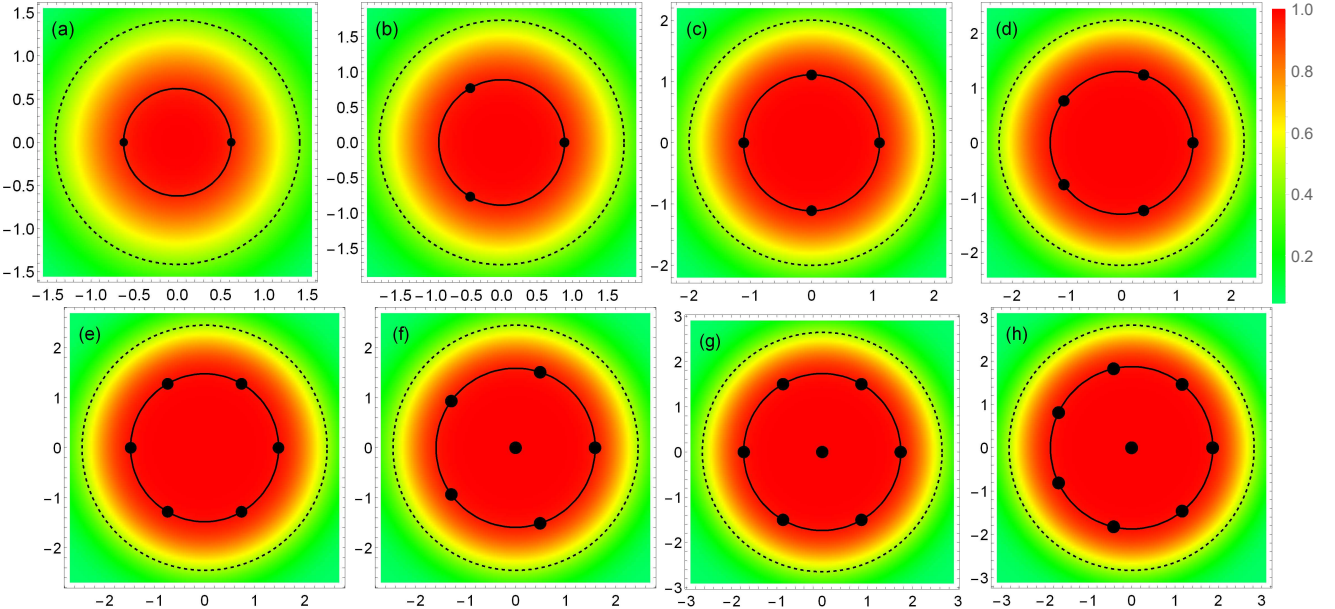


FIG. 5. Configurations of the Wigner crystal molecules in the positive background with the smooth density (12) for $N = 2, \dots, 8$. The color plot shows the positive background density (12). For $N = 2, \dots, 5$ the energy of the single-shell configuration is lower, Figs. (a)-(d). For $N = 7, 8$ the energy of the two-shell configuration, with one electron in the center, is lower, Figs. (g)-(h). For $N = 6$ the single-shell (e) and the two-shell (f) configurations have very close energies.

The potential energy of the positively charged background disk with the density (12) is described by the formula

$$V_b(\mathbf{r}) = \frac{e^2}{a_0} U_N(r/a_0), \quad (57)$$

where

$$U_N(R) = - \sum_{m=0}^{N-1} \frac{(-1)^m N!}{(N-m-1)!(m+1)!m!} \Gamma\left(m + \frac{1}{2}\right) {}_1F_1\left(m + \frac{1}{2}, 1; -R^2\right), \quad (58)$$

and $R = r/a_0$ is the radial coordinate in units a_0 . Now, if a single-shell $(0, N)$ Wigner molecule is considered, the (dimensionless) complex coordinates of electrons can be written as

$$Z_j = Re^{i2\pi(j-1)/N}, \quad j = 1, 2, \dots, N. \quad (59)$$

Then the total energy of the system is

$$E_{(0,N)}(R) = \sum_{j=1}^N U_N(|Z_j|) + \sum_{j=1}^{N-1} \sum_{k=j+1}^N \frac{1}{|Z_j - Z_k|} = N U_N(R) + \frac{1}{R} S_N, \quad (60)$$

where

$$S_N = \sum_{j=1}^{N-1} \sum_{k=j+1}^N \frac{1}{|1 - e^{i2\pi(k-j)/N}|}. \quad (61)$$

In the case of the two-shell Wigner molecule $(1, N-1)$, the particle coordinates are

$$Z_j = Re^{i2\pi(j-1)/(N-1)}, \quad j = 1, 2, \dots, N-1, \quad Z_N = 0 \quad (62)$$

and the total energy has the form

$$E_{(1,N-1)}(R) = (N-1) U_N(R) + U_N(0) + \frac{1}{R} (S_{N-1} + (N-1)). \quad (63)$$

Minimizing the energies (60) and (63) with respect to R one can find the radii of the shells R_N^s in the both types of the molecules and their total energies. The results of such calculations are presented in Table III. One sees that the energy of the $(0, N)$ configuration is smaller than that of the $(1, N-1)$ configuration, if $N \leq 5$. The opposite inequality, $E_{(0,N)} > E_{(1,N-1)}$, is valid at $N \geq 7$. If $N = 6$, the energies of both configurations are very close to each other: the single-shell configuration has slightly lower energy, but the difference is only 0.087%. The N -dependencies of the Wigner molecule energies, for both configurations, are shown in Figure 6. The spatial distribution of the positive background density and the positions of charged point particles in the Wigner molecules are additionally illustrated in Figure 5.

TABLE III. Parameters of Wigner molecules in one-shell $(0, N)$ and two-shell $(1, N-1)$ configurations for $2 \leq N \leq 8$. R_b is the radius of the positively charged background disk, Eq. (11), and R_N^s are the radii of the shells obtained by the minimization of the energies (60) and (63). $E_{(0,N)}/N$ and $E_{(1,N-1)}/N$ are the Wigner molecule energies per particle for two configurations. The lengths are in units a_0 , the energies are in units e^2/a_0 .

N	R_b	Configuration	R_N^s	$E_{(0,N)}/N$	Configuration	R_N^s	$E_{(1,N-1)}/N$
2	1.41421	(0,2)	0.621826	-2.067436			
3	1.73205	(0,3)	0.888015	-2.379006	(1,2)	1.127002	-2.250789
4	2.00000	(0,4)	1.107700	-2.630306	(1,3)	1.282076	-2.553625
5	2.23607	(0,5)	1.301195	-2.841207	(1,4)	1.437241	-2.782655
6	2.44949	(0,6)	1.476787	-3.023620	(1,5)	1.587616	-3.020984
7	2.64575	(0,7)	1.638979	-3.184841	(1,6)	1.732047	-3.206801
8	2.82843	(0,8)	1.790593	-3.329631	(1,7)	1.870522	-3.370707

The quantum-mechanical ground state electron density $n_{\text{GS}}^e(\mathbf{r})$ at $\nu = 1/3$ should be similar to the classical distribution of electrons shown in Figure 5. Therefore, it is to be expected that the function $n_{\text{GS}}^e(\mathbf{r}) = n_{\text{GS}}^e(r)$ should have a maximum at a finite distance $r \simeq R_N^s$ from the disk center, if $N \lesssim 5$, and an additional local maximum at $r = 0$, if $N \gtrsim 6$.

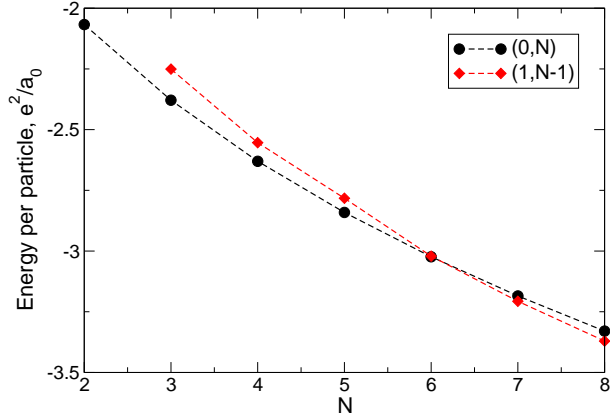


FIG. 6. The energy per particle of the Wigner crystal molecules in the N electron systems for $(0, N)$ configurations at $N = 2, \dots, 8$ and for $(1, N - 1)$ configurations at $N = 3, \dots, 8$.

IV. LAUGHLIN WAVE FUNCTION

We consider the N -electron Laughlin wave function (5) at $m = 3$,

$$\Psi_{\text{RL}} \propto \left(\prod_{1 \leq j < k \leq N} (z_j - z_k)^3 \right) \exp \left(-\frac{1}{2} \sum_{j=1}^N |z_j|^2 \right), \quad (64)$$

which is supposed [7] to be a good approximation to the ground state of the 2DEG at $\nu = 1/3$, and aim to calculate different physical properties of the system in this state. This can be done as follows.

The function (64) is the eigenfunction of the angular momentum operator with the eigenvalue

$$\mathcal{L} = m \frac{N(N-1)}{2} = 3 \frac{N(N-1)}{2}. \quad (65)$$

For any given N and \mathcal{L} we determine N_{mbs} many-body states, formed from the lowest Landau level single-particle functions (8), and expand the Laughlin wave function in these basis states,

$$\Psi_{\text{RL}} = \sum_{s=1}^{N_{\text{mbs}}} A_s \Psi_s. \quad (66)$$

The coefficients A_s here are real numbers, and the function (66) is assumed to be normalized, i.e., $\sum_{s=1}^{N_{\text{mbs}}} A_s^2 = 1$. After the coefficients A_s are found, any physical quantity F can be calculated as the average

$$F = \langle \Psi_{\text{RL}} | \hat{F} | \Psi_{\text{RL}} \rangle = \sum_{s=1}^{N_{\text{mbs}}} \sum_{s'=1}^{N_{\text{mbs}}} A_s A_{s'} \langle \Psi_s | \hat{F} | \Psi_{s'} \rangle. \quad (67)$$

The matrix elements $\langle \Psi_s | \hat{F} | \Psi_{s'} \rangle$ are calculated in Section II E for commonly used operators. This way one can calculate the electron density, energy and other physical properties of the state (64). Let us now calculate the expansion coefficients A_s for the systems with different particle numbers N .

A. Expansion coefficients of the Laughlin function

The coefficients A_s can be found as follows. Using the binomial expansion of the polynomial factors in the Laughlin function, we obtain integer binomial coefficients C_s as in the following example for two particles:

$$(z_1 - z_2)^3 = z_1^3 - 3z_1^2 z_2 + 3z_1 z_2^2 - z_2^3 = (-1)(z_1^0 z_2^3 - z_1^3 z_2^0) + 3(z_1^1 z_2^2 - z_1^2 z_2^1). \quad (68)$$

Since the polynomials in brackets, up to exponential factors, equal the basis functions $|0, 3\rangle$ and $|1, 2\rangle$, the integer numbers

$$C_{|0,3\rangle} = -1 \quad \text{and} \quad C_{|1,2\rangle} = 3 \quad (69)$$

are proportional to the required coefficients $A_{|0,3\rangle}$ and $A_{|1,2\rangle}$. If (for any N) the integers C_s are found, the real coefficients A_s are determined by the normalization condition

$$A_s = \frac{C_s}{\sqrt{\sum_{p=1}^{N_{mbs}} C_p^2}}. \quad (70)$$

1. Two particles

If $N = 2$, then the angular momentum (65) at $\nu = 1/3$ equals $\mathcal{L} = 3$. The number of many-body states in this case is $N_{mbs} = 2$, and they are

$$|0, 3\rangle = \frac{1}{\sqrt{2}} \det \begin{vmatrix} \psi_0(r_1) & \psi_3(r_1) \\ \psi_0(r_2) & \psi_3(r_2) \end{vmatrix}, \quad \text{and} \quad |1, 2\rangle = \frac{1}{\sqrt{2}} \det \begin{vmatrix} \psi_1(r_1) & \psi_2(r_1) \\ \psi_1(r_2) & \psi_2(r_2) \end{vmatrix}, \quad (71)$$

see Table I. Expanding the factor $(z_1 - z_2)^3$ as in (68) we get the coefficients C_s , Eq. (69), and A_s^2 , see Table IV. Notice that two particles are in the state $|1, 2\rangle$ with a much larger probability (90%) than in the state $|0, 3\rangle$ (10%).

TABLE IV. Many-body configurations for $N = 2$ and $\mathcal{L} = 3$ and their weight in the expansion of the Laughlin function.

No.	Configuration	C_s	A_s^2
1	$ 0, 3\rangle$	-1	0.1
2	$ 1, 2\rangle$	3	0.9

2. Three particles

If $N = 3$ then the angular momentum (65) equals $\mathcal{L} = 9$. Now we have $N_{mbs} = 7$ many-body states, see Table II. Using again the binomial expansion

$$(z_1 - z_2)^3(z_1 - z_3)^3(z_2 - z_3)^3 \propto -\Psi_{|0,3,6\rangle} + 3\Psi_{|0,4,5\rangle} + 3\Psi_{|1,2,6\rangle} - 6\Psi_{|1,3,5\rangle} + 15\Psi_{|2,3,4\rangle}. \quad (72)$$

we get the coefficients C_s and A_s^2 presented in Table V. One sees that two of the possible many-body configurations, $|0, 1, 8\rangle$ and $|0, 2, 7\rangle$, are not presented in the Laughlin function (64) at all, while the two states, $|2, 3, 4\rangle$ and $|1, 3, 5\rangle$, take over more than 93% probability. It is also useful to define the quantity

$$P_0(N) = \sum_{s=1}^{N_{mbs}} A_{|0,\dots\rangle}^2 \quad (73)$$

which is the sum of A_s^2 over all many-body configurations, in which one of the particles is in the single-particle state ψ_0 ; this quantity will be used below in Section IV B. In the case of two particles it was $P_0(2) = 10\%$; in the case of three particles it is $P_0(3) = 3.57\%$.

3. Four particles

If $N = 4$, then the total angular momentum (65) equals $\mathcal{L} = 18$, and the number of many-body states is $N_{mbs} = 34$. Applying the binomial expansion procedure we calculate the numbers C_s . Only 16 of them are nonzero; these states,

TABLE V. Many-body configurations for $N = 3$ and $\mathcal{L} = 9$ and their weight in the expansion of the Laughlin function.

No.	Configuration	C_s	A_s^2
1	$ 0, 1, 8\rangle$	0	0
2	$ 0, 2, 7\rangle$	0	0
3	$ 0, 3, 6\rangle$	-1	0.00357
4	$ 0, 4, 5\rangle$	3	0.03214
5	$ 1, 2, 6\rangle$	3	0.03214
6	$ 1, 3, 5\rangle$	-6	0.12857
7	$ 2, 3, 4\rangle$	15	0.80357

their integer weights C_s , as well as the probabilities A_s^2 with which these states are represented in the Laughlin function, are shown in Table VI. Other 18 states, namely

$$\begin{aligned}
&|0, 1, 2, 15\rangle, |0, 1, 3, 14\rangle, |0, 1, 4, 13\rangle, |0, 1, 5, 12\rangle, |0, 1, 6, 11\rangle, |0, 1, 7, 10\rangle, |0, 1, 8, 9\rangle, \\
&|0, 2, 3, 13\rangle, |0, 2, 4, 12\rangle, |0, 2, 5, 11\rangle, |0, 2, 6, 10\rangle, |0, 2, 7, 9\rangle, \\
&|0, 3, 4, 11\rangle, |0, 3, 5, 10\rangle, \\
&|1, 2, 3, 12\rangle, |1, 2, 4, 11\rangle, |1, 2, 5, 10\rangle, \\
&|1, 3, 4, 10\rangle,
\end{aligned}$$

have zero weights C_s . Two many-body configurations out of 34, $|3, 4, 5, 6\rangle$ and $|2, 4, 5, 7\rangle$, contribute almost 85% to the Laughlin function, see Table VI. The probability $P_0(4)$ to have one particle in the single-particle state ψ_0 equals $P_0(4) = 1.82\%$.

TABLE VI. Many-body configurations for $N = 4$ and $\mathcal{L} = 18$, and their weights in the expansion of the Laughlin function.

No.	Configuration	C_s	A_s^2
1	$ 0, 3, 6, 9\rangle$	1	0.000065
2	$ 0, 3, 7, 8\rangle$	-3	0.000584
3	$ 0, 4, 5, 9\rangle$	-3	0.000584
4	$ 0, 4, 6, 8\rangle$	6	0.002338
5	$ 0, 5, 6, 7\rangle$	-15	0.014610
6	$ 1, 2, 6, 9\rangle$	-3	0.000584
7	$ 1, 2, 7, 8\rangle$	9	0.005260
8	$ 1, 3, 5, 9\rangle$	6	0.002338
9	$ 1, 3, 6, 8\rangle$	-12	0.009351
10	$ 1, 4, 5, 8\rangle$	-9	0.005260
11	$ 1, 4, 6, 7\rangle$	27	0.047338
12	$ 2, 3, 4, 9\rangle$	-15	0.014610
13	$ 2, 3, 5, 8\rangle$	27	0.047338
14	$ 2, 3, 6, 7\rangle$	-6	0.002338
15	$ 2, 4, 5, 7\rangle$	-45	0.131494
16	$ 3, 4, 5, 6\rangle$	105	0.715909

In general, as seen from results obtained for two, three and four particles, the largest contribution to the Laughlin function is given by the configurations in which one of the particles has the angular momentum \mathcal{L}/N and the momenta of other particles differ from \mathcal{L}/N by one or two. Indeed, for two particles ($\mathcal{L}/N = 1.5$) the state $|1, 2\rangle$ is the most weighty. If $N = 3$ the state $|2, 3, 4\rangle$ is the most significant, – here the momenta of individual particles are \mathcal{L}/N and $\mathcal{L}/N \pm 1$. The same can be said about the case of $N = 4$. The probability $P_0(N)$ to have one particle in the single-particle state ψ_0 decreases with the growing number of particles N .

4. Five to eight particles

The cases of $N = 5, \dots, 8$ particles can be analyzed similarly. We do not show here full tables of the many-body configurations and their weights, since they are very large; they can be found in Supplementary Materials, see Appendix B. Here, we give a brief summary of the results.

Table VII shows the number of many-body configurations N_{mbs} , the number of states which do not contribute to the Laughlin wave function $N_{mbs}^{=0}$, the number of states which give a nonzero contribution to Ψ_{RL} , $N_{mbs}^{\neq 0}$, and the percentage of many-body configuration *not contributing* to the Laughlin function (64) (denoted as ‘% zero’ in the Table VII). One sees that the number of states not used by the Laughlin wave function dramatically grows with N : while for $N = 3$ ‘only’ 28.57% of all possible many-body configurations are not used, at $N = 8$ it is more than 90.5% of all configurations that are ignored by the Laughlin wave function. This obviously calls into question the Laughlin’s assertion made in Ref. [7] that the wave function of the form (5) ‘has adequate variational freedom’.

TABLE VII. The total number of many-body states N_{mbs} , the number of states contributing ($N_{mbs}^{\neq 0}$) and not contributing ($N_{mbs}^{=0}$) to the Laughlin function, as well as the percentage of non-contributing many-body configurations (‘% zero’). N is the number of particles and \mathcal{L} is the total angular momentum (65) corresponding to $\nu = 1/3$ and $m = 3$ in Eq. (5).

N	\mathcal{L}	N_{mbs}	$N_{mbs}^{=0}$	$N_{mbs}^{\neq 0}$	% zero
2	3	2	0	2	00.00
3	9	7	2	5	28.57
4	18	34	18	16	52.94
5	30	192	133	59	69.27
6	45	1206	959	247	79.52
7	63	8033	6922	1111	86.17
8	84	55974	50680	5294	90.54

Tables VIII, IX, X, and XI show the most weighty configurations contributing to the Laughlin function for $N = 5, 6, 7$, and 8. One sees, again, that in each case only two configurations out of hundreds and thousands give the most significant contribution to the Laughlin function. The probability $P_0(N)$ equals $P_0(5) = 1.10\%$ in the case $N = 5$, $P_0(6) = 0.735\%$ at $N = 6$, $P_0(7) = 0.526\%$ at $N = 7$, and $P_0(8) = 0.395\%$ at $N = 8$.

TABLE VIII. Many-body configurations contributing the largest weights ($|C_s| \geq 180$) in the expansion of the Laughlin function, for $N = 5$ and $\mathcal{L} = 30$.

No.	Configuration	C_s	A_s^2
36	$ 1, 5, 7, 8, 9\rangle$	-180	0.023120
52	$ 2, 5, 6, 8, 9\rangle$	270	0.052019
54	$ 3, 4, 5, 7, 11\rangle$	-180	0.023120
56	$ 3, 4, 6, 7, 10\rangle$	270	0.052019
58	$ 3, 5, 6, 7, 9\rangle$	-420	0.125874
59	$ 4, 5, 6, 7, 8\rangle$	945	0.637238

TABLE IX. Many-body configurations contributing the largest weights ($|C_s| \geq 2250$) in the expansion of the Laughlin function, for $N = 6$ and $\mathcal{L} = 45$.

No.	Configuration	C_s	A_s^2
201	$ 2, 6, 7, 9, 10, 11\rangle$	-2250	0.026562
236	$ 3, 6, 7, 8, 10, 11\rangle$	3150	0.052062
241	$ 4, 5, 6, 8, 9, 13\rangle$	-2250	0.026562
244	$ 4, 5, 7, 8, 9, 12\rangle$	3150	0.052062
246	$ 4, 6, 7, 8, 9, 11\rangle$	-4725	0.117139
247	$ 5, 6, 7, 8, 9, 10\rangle$	10395	0.566954

Having obtained the expansion coefficients C_s we can now calculate different physical properties of the Laughlin function (64). We begin with the density of electrons in the Laughlin state (64).

TABLE X. Many-body configurations contributing the largest weights ($|C_s| \geq 31500$) in the expansion of the Laughlin function, for $N = 7$ and $\mathcal{L} = 63$.

No.	Configuration	C_s	A_s^2
1025	$ 3, 7, 8, 9, 11, 12, 13\rangle$	-31500	0.027401
1096	$ 4, 7, 8, 9, 10, 12, 13\rangle$	42525	0.049938
1105	$ 5, 6, 7, 9, 10, 11, 15\rangle$	-31500	0.027401
1108	$ 5, 6, 8, 9, 10, 11, 14\rangle$	42525	0.049938
1110	$ 5, 7, 8, 9, 10, 11, 13\rangle$	-62370	0.107423
1111	$ 6, 7, 8, 9, 10, 11, 12\rangle$	135135	0.504291

TABLE XI. Many-body configurations contributing the largest weights ($|C_s| \geq 496125$) in the expansion of the Laughlin function, for $N = 8$ and $\mathcal{L} = 84$.

No.	Configuration	C_s	A_s^2
5138	$ 4, 8, 9, 10, 11, 13, 14, 15\rangle$	-496125	0.026866
5272	$ 5, 8, 9, 10, 11, 12, 14, 15\rangle$	654885	0.046812
5288	$ 6, 7, 8, 10, 11, 12, 13, 17\rangle$	-496125	0.026866
5291	$ 6, 7, 9, 10, 11, 12, 13, 16\rangle$	654885	0.046812
5293	$ 6, 8, 9, 10, 11, 12, 13, 15\rangle$	-945945	0.097669
5294	$ 7, 8, 9, 10, 11, 12, 13, 14\rangle$	2027025	0.448480

B. Electron density in the Laughlin state

The matrix elements of the density operator (28) are diagonal, therefore, the function $n_e(\mathbf{r})$ can be written as

$$n_e(\mathbf{r}) = \sum_{s=1}^{N_{mbs}} A_s^2 \langle \Psi_s | \hat{n}_e(\mathbf{r}) | \Psi_s \rangle = n_s \frac{1}{\nu} \sum_{s=1}^{N_{mbs}} A_s^2 \sum_{i=1}^N \frac{1}{L_i^{(s)}!} \left(\frac{r}{\lambda} \right)^{2L_i^{(s)}} \exp \left(-\frac{r^2}{\lambda^2} \right), \quad (74)$$

where $\nu = 1/m = 1/3$. Substituting into Eq. (74) the coefficients A_s^2 , found in the previous Section, we calculate the density of electrons in the N -particle systems, with N varying from 2 to 8. The result is shown in Figure 7 by solid curves; the corresponding densities of the positive background are shown by dashed curves. One sees that, while the positive background density is constant in the bulk of the disk and falls down at its boundary, the Laughlin state density is strongly inhomogeneous: it has the shape of a ring, with a much smaller density than $n_b(r)$ in the disk center, and with a much larger density than $n_b(r)$ near the edge of the disk. If $N \leq 5$, the shape of the Laughlin density $n_e(r)$ can still be considered as reasonable: according to the expectations, discussed in Section III B, the Wigner molecule in this case has a single shell so that the density maximum is expected at a finite distance from the center. But at $N \geq 6$ an additional electron appears in the center of the Wigner molecule, Fig. 5(f,g,h), so that a local maximum at $r = 0$ should appear in the electron density dependence of the true ground state of the system. This is not the case for the Laughlin wave function.

The density of electrons at $r = 0$ is determined by the many-body configurations of the type $|0, \dots\rangle$, in which one of electrons occupies the single-particle state $|0\rangle = \psi_0(\mathbf{r})$. As seen from (74),

$$\frac{n_e(0)}{n_s} = \frac{1}{\nu} \sum_{s=1}^{N_{mbs}} A_s^2 \sum_{i=1}^N \delta_{L_i^{(s)}, 0} = \frac{1}{\nu} P_0(N). \quad (75)$$

As we have seen in Section IV A, the vast majority of this type of configurations have zero weight in the Laughlin function. Those that survived, like the first five configurations in Table VI, have very low weight leading to $P_0(N)$ less than 1% for $N > 5$. As a result, the density of electrons in the disk center is much smaller than the density of the positive background, with the ratio $n_e(0)/n_s$ tending to zero at $N \rightarrow \infty$. Figure 8 shows the dependence of $n_e(0)/n_s$ on the number of particles for the Laughlin state. In the investigated range $2 \leq N \leq 8$ this dependence is very well fitted by the curve

$$\frac{n_e(0)}{n_s} \approx \frac{A}{N^{7/3}}, \quad (76)$$

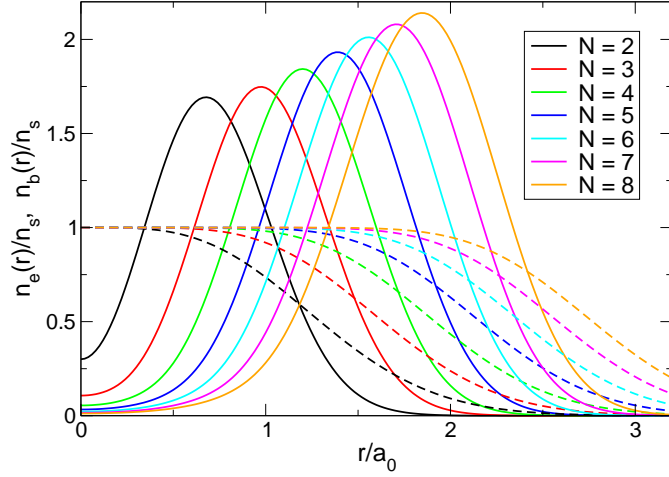


FIG. 7. The density of electrons (solid curves) in the Laughlin state (64) as a function of the radial coordinate for $N = 2 - 8$. The dashed curves show the corresponding positive background densities.

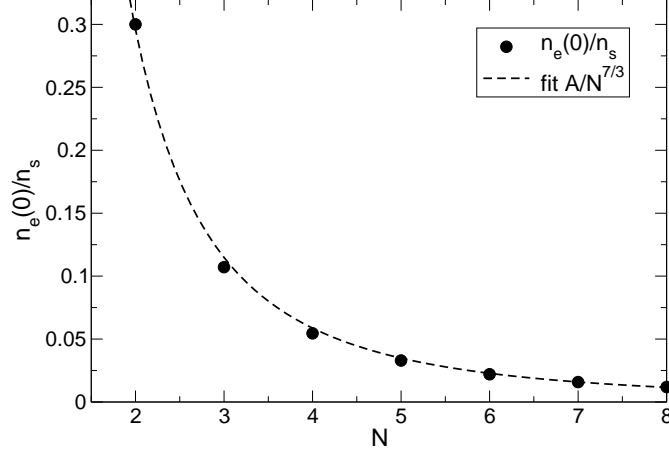


FIG. 8. The Laughlin density of electrons at $r = 0$ (symbols) and the fit $A/N^{7/3}$ with $A = 1.4912$, as a function of the number of particles N .

where $A = 1.4912$ gives the best fit to the calculated points. Near the edge, in the point $r = R_{\max}$ of the density maximum, the ratio $n_e(R_{\max})/n_s$ tends to infinity in the thermodynamic limit $N \rightarrow \infty$.

Thus, the Laughlin wave function (64) describes not a uniform liquid, but a fictitious strongly inhomogeneous ring-shaped state which cannot exist in nature.

C. Energy of the Laughlin state

For completeness let us now calculate the energy of the Laughlin state. As we have mentioned in Introduction, Laughlin implicitly assumed in [7] that the density of electrons in his state is uniform and calculated only the correlation contribution. However, a correct calculation should include the full Coulomb energy (17), with background-background, background-electron and electron-electron interactions $\hat{V}_{bb} + \hat{V}_{eb} + \hat{V}_{ee}$. The energy of the Laughlin state is then determined by the formula

$$E_{RL} = \langle \Psi_{RL} | \hat{\mathcal{H}} | \Psi_{RL} \rangle = \sum_{s=1}^{N_{mbs}} \sum_{s'=1}^{N_{mbs}} A_s A_{s'} \langle \Psi_s | \hat{\mathcal{H}} | \Psi_{s'} \rangle = \frac{\sum_{s=1}^{N_{mbs}} \sum_{s'=1}^{N_{mbs}} C_s C_{s'} \langle \Psi_s | \hat{V}_{bb} + \hat{V}_{eb} + \hat{V}_{ee} | \Psi_{s'} \rangle}{\sum_{p=1}^{N_{mbs}} C_p^2} \quad (77)$$

(we omit the kinetic energy $\hbar\omega_c/2$ per particle). The integer numbers C_s – the expansion coefficients of the Laughlin wave function over the basis states (20) – have been found in Section IV A. The matrix elements of the background-

background, background-electron and electron-electron interactions have been calculated in Section II E. The energy of the Laughlin state (64) can therefore be calculated exactly using the formula (77). We have done this for N up to eight particles. The results will be shown in the next Section, together with the exact results for the ground state energy.

V. EXACT SOLUTION

Now we can analyze the true ground state of the system of N interacting particle on a neutralizing positive background.

A. The ground state energy and wave function

The ground and excited states energies, as well the eigenvectors A_s can be found by solving the eigenvalue problem (50). All many-body matrix elements required for the Hamiltonian matrix in (50) have been calculated in Section II E, so that the problem can be easily solved, at least for a moderate number of particles. We have found the exact solution of the problem for $2 \leq N \leq 7$. The case of seven particles reproduces a small piece of the macroscopic Wigner crystal, Fig. 5(g), therefore, results for $N = 7$ are most important for understanding the physics of the considered systems.

Table XII shows our results for the exact ground state energy E_{GS}/N at $\nu = 1/3$, and the Laughlin state energy E_{RL}/N , in units of e^2/a_0 . Two right columns in Table XII give the difference between E_{GS}/N and E_{RL}/N , in absolute values and in percents. Figure 9 illustrates the N -dependencies of both energies.

TABLE XII. Energy per particle of the exact ground state E_{GS}/N and the Laughlin state E_{RL}/N , in units e^2/a_0 , for different numbers of particles N . $\Delta E = E_{\text{RL}} - E_{\text{GS}}$ is the difference between the two energies in units e^2/a_0 and “ ΔE in %” is the difference in percents.

N	E_{GS}/N	E_{RL}/N	$\Delta E/N$	ΔE in %
2	-0.908604	-0.899355	0.0092	1.018
3	-0.927039	-0.915443	0.0116	1.251
4	-0.937894	-0.923384	0.0145	1.547
5	-0.943111	-0.923967	0.0191	2.030
6	-0.946922	-0.919313	0.0276	2.916
7	-0.951626	-0.911038	0.0406	4.265
8	—	-0.900274	—	—

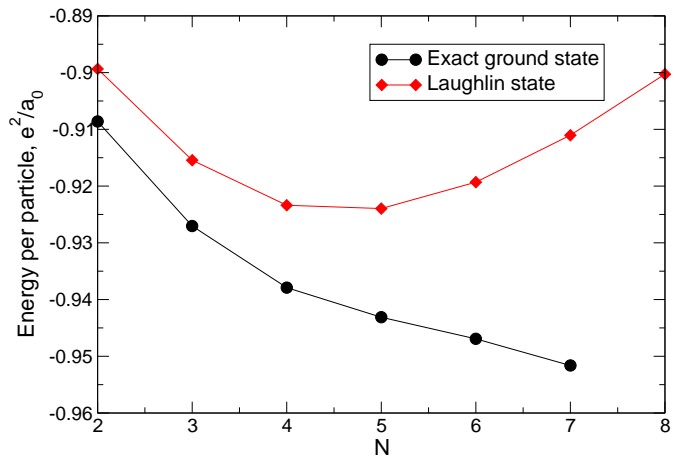


FIG. 9. The exact ground state and Laughlin state energies (per particle) as a function of the number of particles N . The energies are in units e^2/a_0 .

The exact ground state energy is about $-0.91e^2/a_0$ at $N = 2$ and then monotonously decreases with N , similar to the energy of the MDD state, Fig. 4, and of the classical Wigner crystal configuration, Fig. 6. The point at $N = 7$ lies slightly lower than one would expect from the tendency seen on the way from two to six particles which is evidently due to the fact the Wigner molecule at $N = 7$ represents the most dense (triangular lattice) packing on a 2D plane.

The Laughlin energy (per particle) is about 1% higher than the exact energy at $N = 2$ and then also goes down at $N = 3$ and 4. However, the deviation from the exact energy increases, and starting from $N = 5$ the Laughlin energy starts to grow with increasing N . This behavior is easy to understand keeping in mind that the density of electrons in the Laughlin state has the ring form *at all* N , so that the difference between the background and electron densities becomes very large at $N \gtrsim 6$, Fig. 7 and continues to grow at $N \rightarrow \infty$.

The eigenvectors A_s are quite different for the exact ground and Laughlin states. As examples, we compare the coefficients A_s for two and three particles in Tables XIII and XIV. One sees that the Laughlin function overestimates the weight of the higher states, $|1, 2\rangle$ and $|2, 3, 4\rangle$, which mainly contribute to the electron density at $r \simeq R$, and underestimates the weight of the lower states, $|0, 3\rangle$ and $|0, 1, 8\rangle$, contributing to the density at $r = 0$. This fact has been already discussed in Section IV B; the same tendency is also the case at other numbers of particles.

TABLE XIII. The expansion coefficients A_s for the exact ground state and the Laughlin wave function, for the case of $N = 2$ particles.

s	state	A_s^{RL}	A_s^{GS}
1	$ 0, 3\rangle$	-0.31623	-0.51276
2	$ 1, 2\rangle$	0.948683	0.85853

TABLE XIV. The expansion coefficients A_s for the exact ground state and the Laughlin wave function, for the case of $N = 3$ particles.

s	state	A_s^{RL}	A_s^{GS}
1	$ 0, 1, 8\rangle$	0	0.03122
2	$ 0, 2, 7\rangle$	0	-0.05843
3	$ 0, 3, 6\rangle$	-0.05976	-0.10431
4	$ 0, 4, 5\rangle$	0.17928	0.35338
5	$ 1, 2, 6\rangle$	0.17928	0.33418
6	$ 1, 3, 5\rangle$	-0.35857	-0.46311
7	$ 2, 3, 4\rangle$	0.89642	0.73056

To characterize further the deviation of the exact ground state wave function from the Laughlin one we calculate the projection of the functions Ψ_{RL} on Ψ_{GS} ,

$$\langle \Psi_{\text{RL}} | \Psi_{\text{GS}} \rangle = \sum_{s=1}^{N_{\text{mbs}}} A_s^{\text{RL}} A_s^{\text{GS}}. \quad (78)$$

The Table XV and Figure 10 show the results. At $N = 2$ and $N = 3$ the values (78) are sufficiently close to unity, but then dramatically fall down achieving the value ~ 0.38 for seven particles.

TABLE XV. The projections of the Laughlin wave function on the exact ground state wave function at $\nu = 1/3$.

N	$\langle \Psi_{\text{RL}} \Psi_{\text{GS}} \rangle$
2	0.97662424
3	0.95044339
4	0.90858482
5	0.82307942
6	0.62939553
7	0.38458980

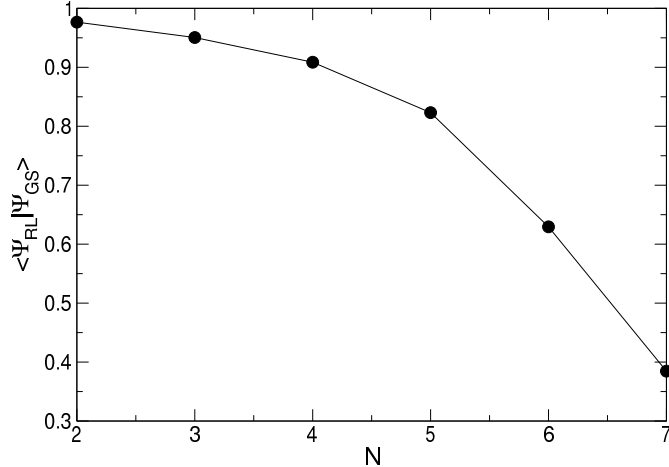


FIG. 10. The projection (78) of the Laughlin wave function on the exact ground state wave function at $\nu = 1/3$ as a function of N .

B. The density of electrons in the ground state

The density of electrons in the exact ground states in systems with different N can be calculated using the matrix elements (28) and the expansion coefficients of the exact ground state wave function A_s^{GS} ,

$$n_e^{\text{GS}}(r) = \sum_{s=1}^{N_{\text{mbs}}} (A_s^{\text{GS}})^2 \sum_{j=1}^N |\psi_{L_j^{(s)}}(\mathbf{r})|^2. \quad (79)$$

The results of calculations are shown in Figure 11 for N from 2 to 7. Shown are the densities of the positive background (black solid curve), of electrons in the Laughlin (red dashed) and in the exact ground state (blue dot-dashed curve). Comparing now the behavior of the red and blue curves one can understand the physics of the ground state and the problems of the Laughlin function.

Consider first the cases of a small number of particles, $2 \leq N \leq 4$. At large distances from the center the Laughlin and exact densities are very close to each other. The difference is evident at small r . If $N = 2$ the (dimensionless) density of electrons in the ground state is about 0.79, which is 2.6 times larger than that of the Laughlin state (0.3). So, the Laughlin electrons avoid the center much stronger than it is required by the Coulomb repulsion forces. Three particles stronger repel each other, therefore the maximum of both densities at $N = 3$ moves to a larger radius, and the density in the center further decreases. However, the Laughlin density (~ 0.1) is again much smaller than the exact electron density (~ 0.42) at $r = 0$, this time by a factor of 4.2. At $N = 4$ this tendency further increases: the Laughlin density is ~ 0.0545 , which is 6.4 times smaller than the exact density (0.35) at $r = 0$.

When N becomes equal to 5 and more, the behavior of the exact and Laughlin density at $r = 0$ acquire opposite tendencies. The Laughlin density in the disk center continues to fall down. In contrast, the ground state density of the exact solution begins to grow. As seen from the classical Wigner crystal configurations, Fig. 5, one electron appears in the disk center at $N = 6$, but this tendency begins to manifest itself already at $N = 5$. The exact density of electrons at $r = 0$ equals 0.49 at $N = 5$, while the Laughlin density falls down to ~ 0.033 . At $N = 6$ $n_e(r)/n_s$ equals 0.996 – one electron appears in the center. Finally, at $N = 7$ the density of electrons at $r = 0$ equals 1.585, which is even larger than the maximum at the finite $r/a_0 = 1.84$, that equals 1.516. But the Laughlin density continues to fall down in the disk center.

Thus, the exact solution clearly shows that the ground state of a few-electron system represents a Wigner-crystal-type structure, with positions of electrons averaged over the polar angle – a floating Wigner crystal state [12–16]. This agrees with an intuitive understanding of the physics of Coulomb-interacting particles and restores the “historical injustice” committed against the Wigner crystal in 1983 [8].

VI. CONCLUSIONS

We have investigated ground state properties of a system of a few (up to seven) Coulomb interacting electrons on the neutralizing positive background of the disk shape, in the presence of the external magnetic field corresponding to

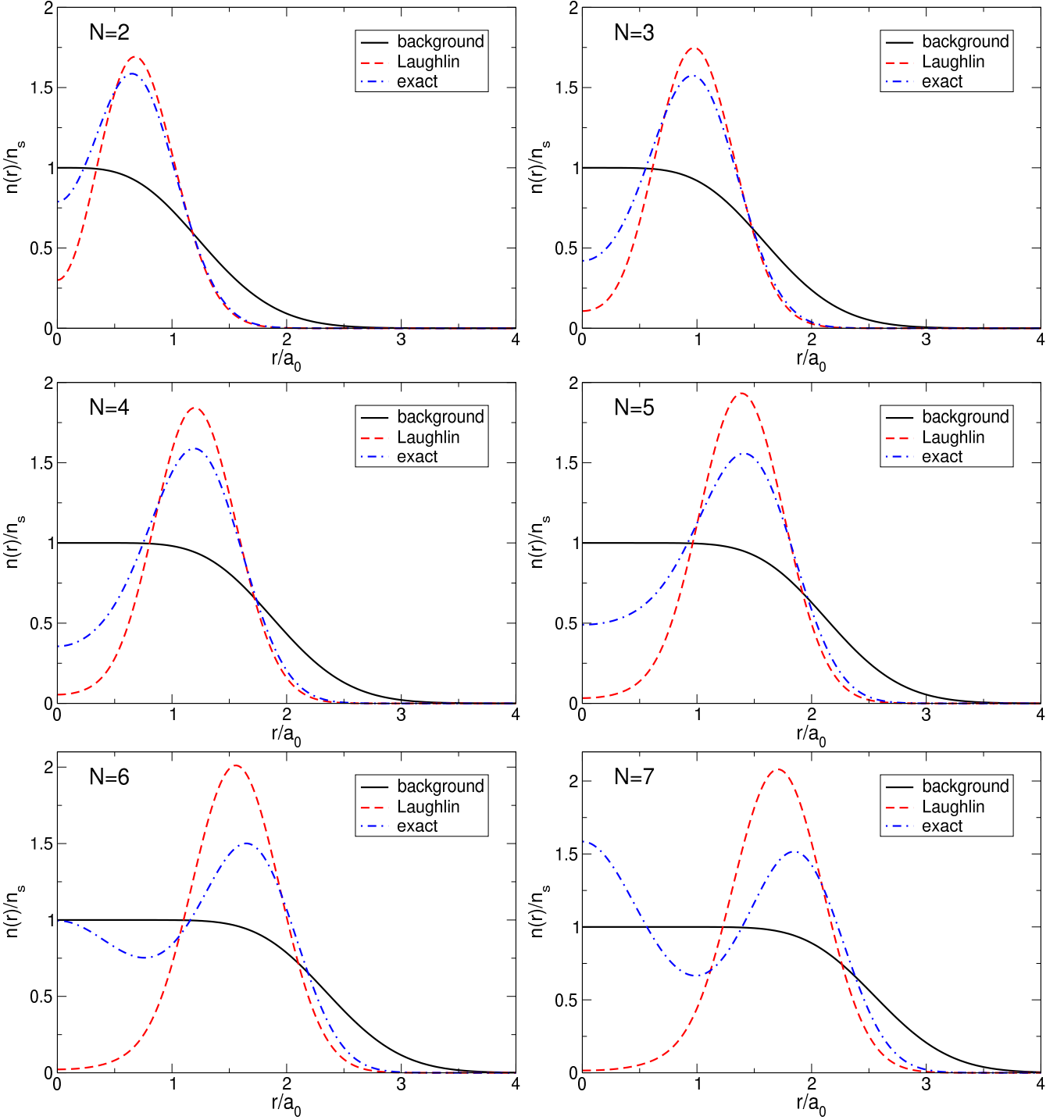


FIG. 11. The density of the positive background and electrons in the exact ground state and in the Laughlin state at different numbers of particles.

the Landau level filling factor $\nu = 1/3$. We have shown that the ground state of the system has the form of a sliding Wigner molecule corresponding to a classical distribution of point charges with the positions averaged over the polar angle, to restore the rotational symmetry of the system.

We have analyzed the physical properties of the Laughlin function (5) which was proposed in 1983 as a variational wave function for the ground state of the considered system. We have shown that the density of electrons in the state (5) is strongly inhomogeneous and has the shape of a ring with the maximum electron density at the edge of the

positively charged disk and with a deep hole in the disk center. The Laughlin calculations of the energy of the state (5) were erroneous since they did not take into account that the local electroneutrality condition is strongly violated in the state (5). Thus, the “new state of matter” [7] – the incompressible quantum liquid with fractionally charged quasi-particles – does not represent any real physical system.

Appendix A: Integrals \mathcal{J} and \mathcal{K}

In order to present the Coulomb interaction matrix elements in a simple and universal form, we introduce two integrals, \mathcal{J} and \mathcal{K} . The integral \mathcal{J} is defined as follows

$$\mathcal{J}(n_1, n_2, l_1, l_2, k; \alpha, \beta) = \sqrt{\frac{8}{\pi}} \int_0^\infty dx x^{2k} L_{n_1}^{l_1}(\alpha x^2) L_{n_2}^{l_2}(\beta x^2) e^{-(\alpha+\beta)x^2}, \quad (\text{A1})$$

where n_1, n_2, l_1, l_2 , and k are integers, α, β are real numbers, and $L_n^l(x)$ are Laguerre polynomials. Substituting the explicit expression for the generalized Laguerre polynomial

$$L_n^l(x) = \sum_{m=0}^n (-1)^m \frac{(n+l)!}{(n-m)!(m+l)!} \frac{x^m}{m!} \quad (\text{A2})$$

into the definition (A1) we get a finite sum of integrals of the type $\int_0^\infty x^{2n} e^{-ax^2} dx$, which can be analytically calculated. The final result is

$$\mathcal{J}(n_1, n_2, l_1, l_2, k; \alpha, \beta) = \sqrt{\frac{2}{\alpha+\beta}} \sum_{m_1=0}^{n_1} \frac{(-1)^{m_1} (n_1 + l_1)!}{(n_1 - m_1)!(m_1 + l_1)!} \frac{\alpha^{m_1}}{m_1!} \sum_{m_2=0}^{n_2} \frac{(-1)^{m_2} (n_2 + l_2)!}{(n_2 - m_2)!(m_2 + l_2)!} \frac{\beta^{m_2}}{m_2!} \frac{[2(m_1 + m_2 + k) - 1]!!}{[2(\alpha + \beta)]^{m_1 + m_2 + k}}. \quad (\text{A3})$$

The matrix elements of the electron-electron interaction are expressed in terms of the integrals \mathcal{J} with the real arguments $\alpha = \beta = 1$. For them we define another integral,

$$\mathcal{K}(n_1, n_2, k) = \sqrt{\frac{n_1!}{(n_1 + k)!} \frac{n_2!}{(n_2 + k)!}} \mathcal{J}(n_1, n_2, k, k, k; 1, 1), \quad (\text{A4})$$

which depends only on three integer arguments.

Appendix B: Supplementary Materials

The directory **Supplementary Materials** supplied together with the paper contains seven subdirectories $N=2$, $N=3$, ..., and $N=8$. Each subdirectory has three files named like $\dots.N=7.Ltot=63.dat$. The file names contain information about the number of particles N and the total angular momentum $\mathcal{L} = 3N(N-1)/2$ corresponding to $\nu = 1/3$. These files contain the following information:

1. file **Nmbs.N=7.Ltot=63.dat** contains a single number, which is the number of many-body states N_{mbs} for given N and \mathcal{L} ; for example, for $N = 7$ it is 8033
2. file **MBstates.N=7.Ltot=63.dat** contains N_{mbs} many-body states; for example, for $N = 7$ these are the states running from the state number 1, $|0, 1, 2, 3, 4, 5, 48\rangle$, up to the state number 8033, $|6, 7, 8, 9, 10, 11, 12\rangle$
3. file **LaughlinWeights.N=7.Ltot=63.dat** contains the integer numbers C_s of the expansion of Laughlin function over the basis many-body states, see Section IV A; for example, for $N = 7$ and for the first and the last basis many-body states these are $C_{|0,1,2,3,4,5,48\rangle} = 0$ and $C_{|6,7,8,9,10,11,12\rangle} = 135135$.

Using the provided information the reader may reproduce our results for the density and the energy of the Laughlin state (64).

[1] K. von Klitzing, G. Dorda, and M. Pepper, New method for high-accuracy determination of the fine-structure constant based on quantized Hall resistance, *Phys. Rev. Lett.* **45**, 494 (1980).

- [2] R. E. Prange and S. M. Girvin, eds., *The Quantum Hall Effect* (Springer, New York, 1990).
- [3] D. C. Tsui, H. L. Stormer, and A. C. Gossard, Two-dimensional magnetotransport in the extreme quantum limit, *Phys. Rev. Lett.* **48**, 1559 (1982).
- [4] R. Willett, J. P. Eisenstein, H. L. Stormer, D. C. Tsui, A. C. Gossard, and J. H. English, Observation of an even-denominator quantum number in the fractional quantum Hall effect, *Phys. Rev. Lett.* **59**, 1776 (1987).
- [5] K. I. Bolotin, F. Ghahari, M. D. Shulman, H. L. Stormer, and P. Kim, Observation of the fractional quantum Hall effect in graphene, *Nature* **462**, 196 (2009).
- [6] E. Wigner, On the interaction of electrons in metals, *Phys. Rev.* **46**, 1002 (1934).
- [7] R. B. Laughlin, Anomalous quantum Hall effect: An incompressible quantum liquid with fractionally charged excitations, *Phys. Rev. Lett.* **50**, 1395 (1983).
- [8] K. Maki and X. Zotos, Static and dynamic properties of a two-dimensional Wigner crystal in a strong magnetic field, *Phys. Rev. B* **28**, 4349 (1983).
- [9] R. Tao, Comment on Laughlin's wavefunction for the quantised Hall effect, *J. Phys. C: Solid State Phys.* **17**, L53 (1984).
- [10] <https://www.nobelprize.org/prizes/physics/1998/summary/>.
- [11] Y. A. Bychkov, S. V. Iordanskii, and G. M. Eliashberg, Two-dimensional electrons in a strong magnetic field, *JETP Lett.* **33**, 143 (1981).
- [12] S. A. Mikhailov and K. Ziegler, Floating Wigner molecules and possible phase transitions in quantum dots, *European Physical Journal B* **28**, 117 (2002).
- [13] C. Yannouleas and U. Landman, Two-dimensional quantum dots in high magnetic fields: Rotating-electron-molecule versus composite-fermion approach, *Phys. Rev. B* **68**, 035326 (2003).
- [14] C. Yannouleas and U. Landman, Symmetry breaking and quantum correlations in finite systems: studies of quantum dots and ultracold Bose gases and related nuclear and chemical methods, *Rep. Prog. Phys.* **70**, 2067–2148 (2007).
- [15] M. Lewin, E. H. Lieb, and R. Seiringer, Statistical mechanics of the uniform electron gas, *Journal de l'École polytechnique — Mathématiques* **5**, 79 (2018).
- [16] M. Lewin, E. H. Lieb, and R. Seiringer, Floating Wigner crystal with no boundary charge fluctuations, *Phys. Rev. B* **100**, 035127 (2019).